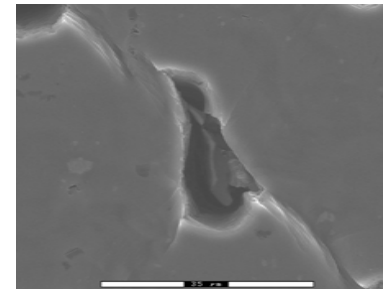
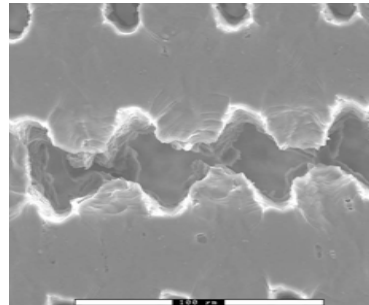


1. Institute of Mechanics, Materials and Civil Engineering (iMMC), Université catholique de Louvain, Belgium
2. Laboratoire MATEIS, Département SGM, INSA Lyon, France
3. Department of Mechanical Engineering, TOBB University of Economics and Technology, Ankara, Turkey
4. Institut Jean-Le-Rond-d'Alembert, Université Paris VI, France
5. Zernike Institute, University of Groningen, The Netherlands

## **Void coalescence modelling : strain hardening, second population and shear effects**

**T. Pardoen<sup>1</sup>, L. Lecarme<sup>1</sup>, F. Scheyvaerts<sup>1</sup>, D. Fabrègue<sup>2</sup>,  
C. Tekoğlu<sup>3</sup>, J.-B. Leblond<sup>4</sup>, P. Onck<sup>4</sup>**



**MECAMAT – Journée du GT MECAMAT « Physique et Mécanique de  
l'Endommagement et de la Rupture »**  
***Modélisation et simulation de la rupture ductile : synthèse des connaissances  
et questions d'enjeux***  
**Mardi 25 septembre 2012, EDF R&D, Clamart, France**

# OUTLINE

- 1. Experimental observations**
- 2. « Elementary » models for the onset of void coalescence**
- 3. Fine tuning of Thomason model**
- 4. Extension to strain hardening**
- 5. Extension to a second population**
- 6. Extension to combined shear/tension coalescence**
- 7. Models for the coalescence stage**

# OUTLINE

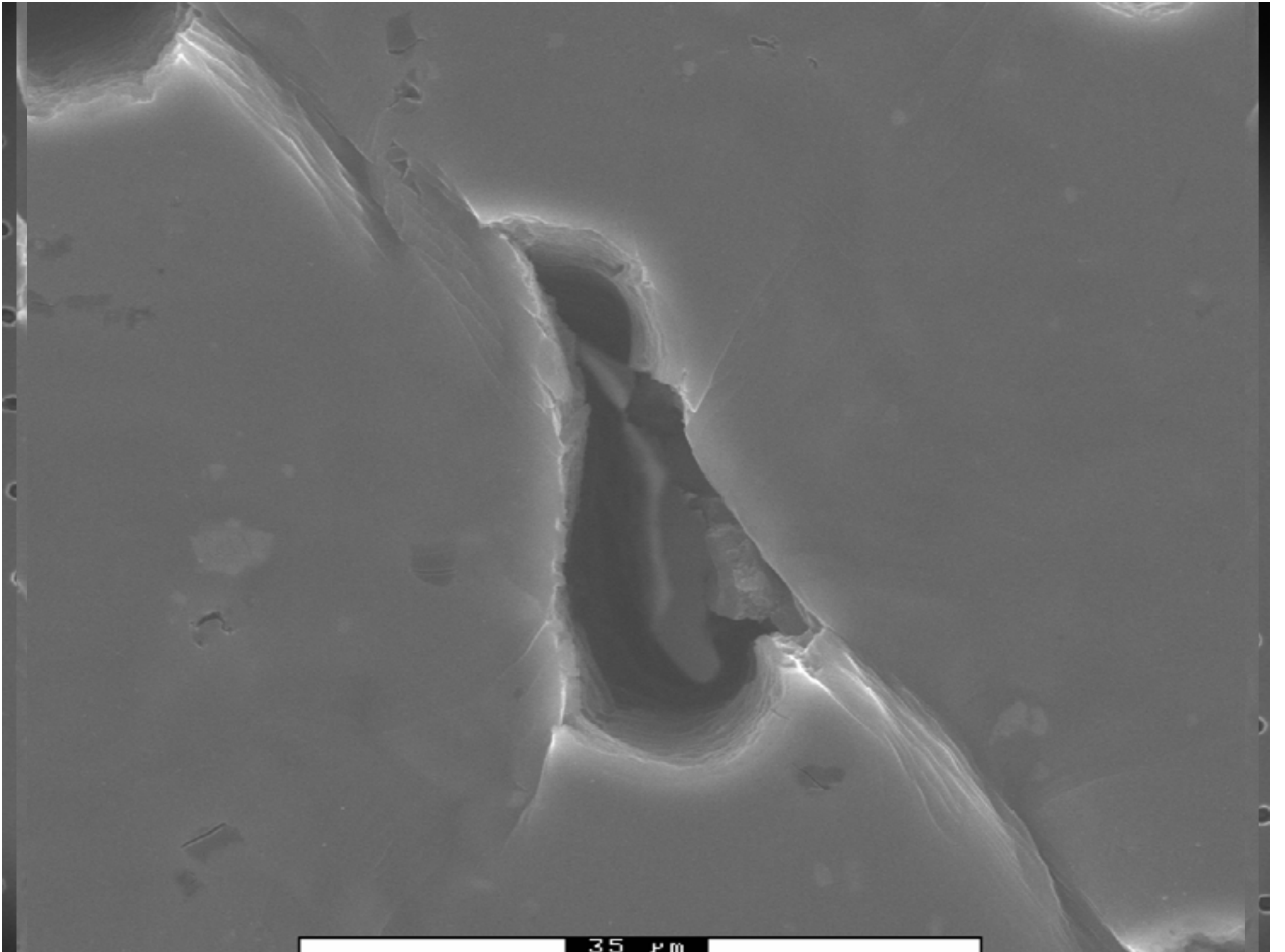
- 1. Experimental observations**
2. « Elementary » models for the onset of void coalescence
3. Fine tuning of Thomason model
4. Extension to strain hardening
5. Extension to a second population
6. Extension to combined shear/tension coalescence
7. Models for the coalescence stage

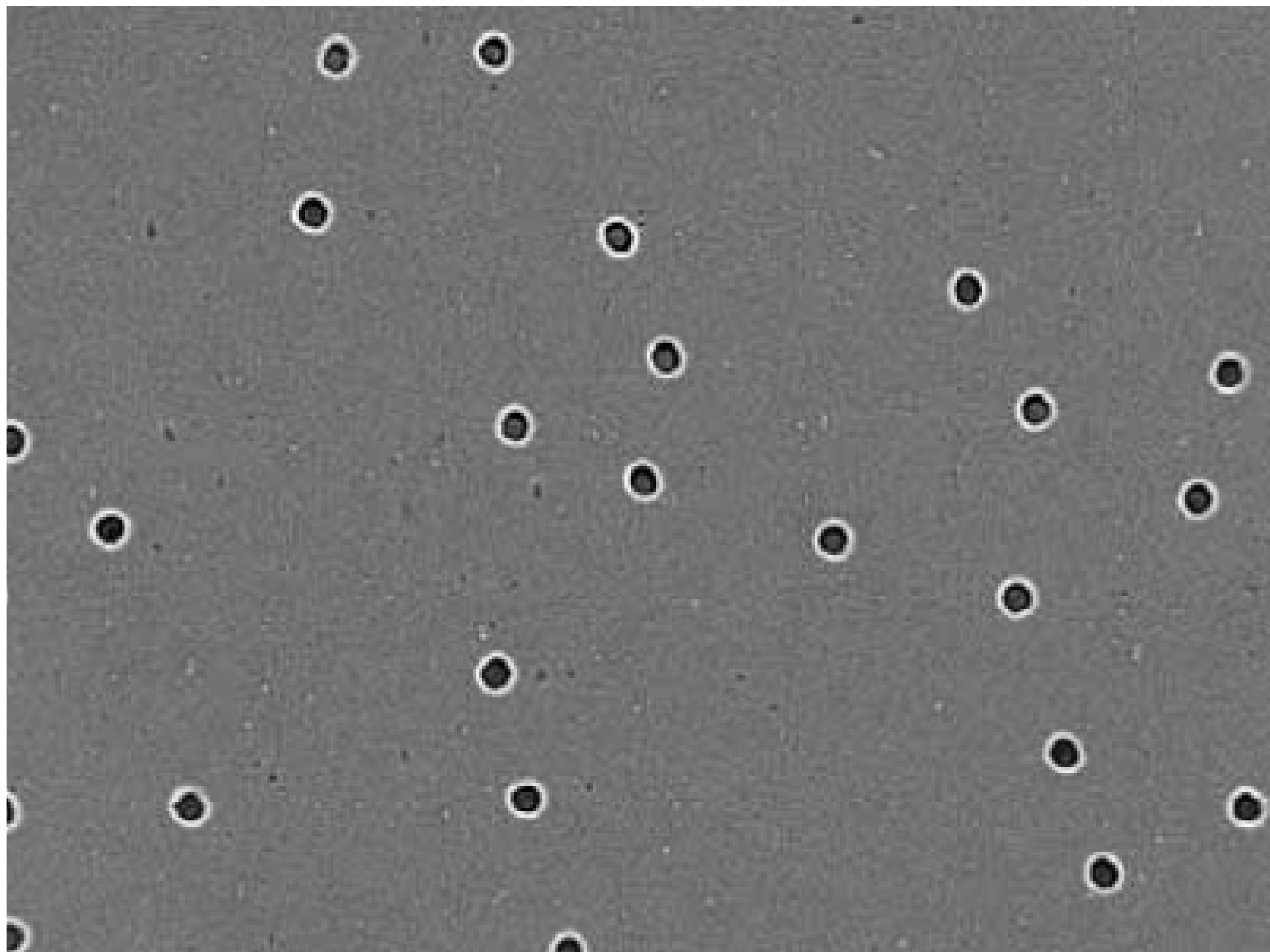


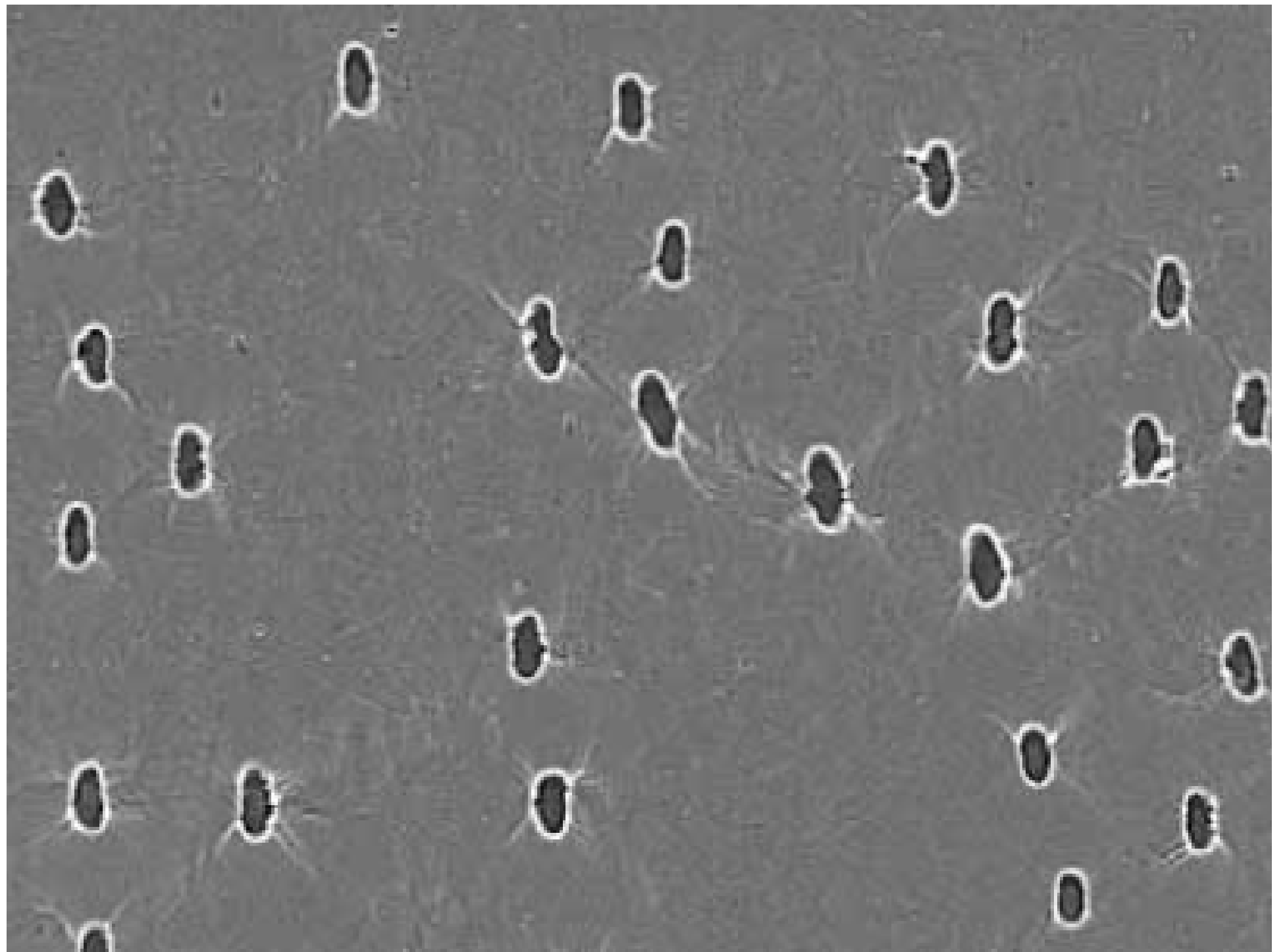
# Void coalescence – experiments

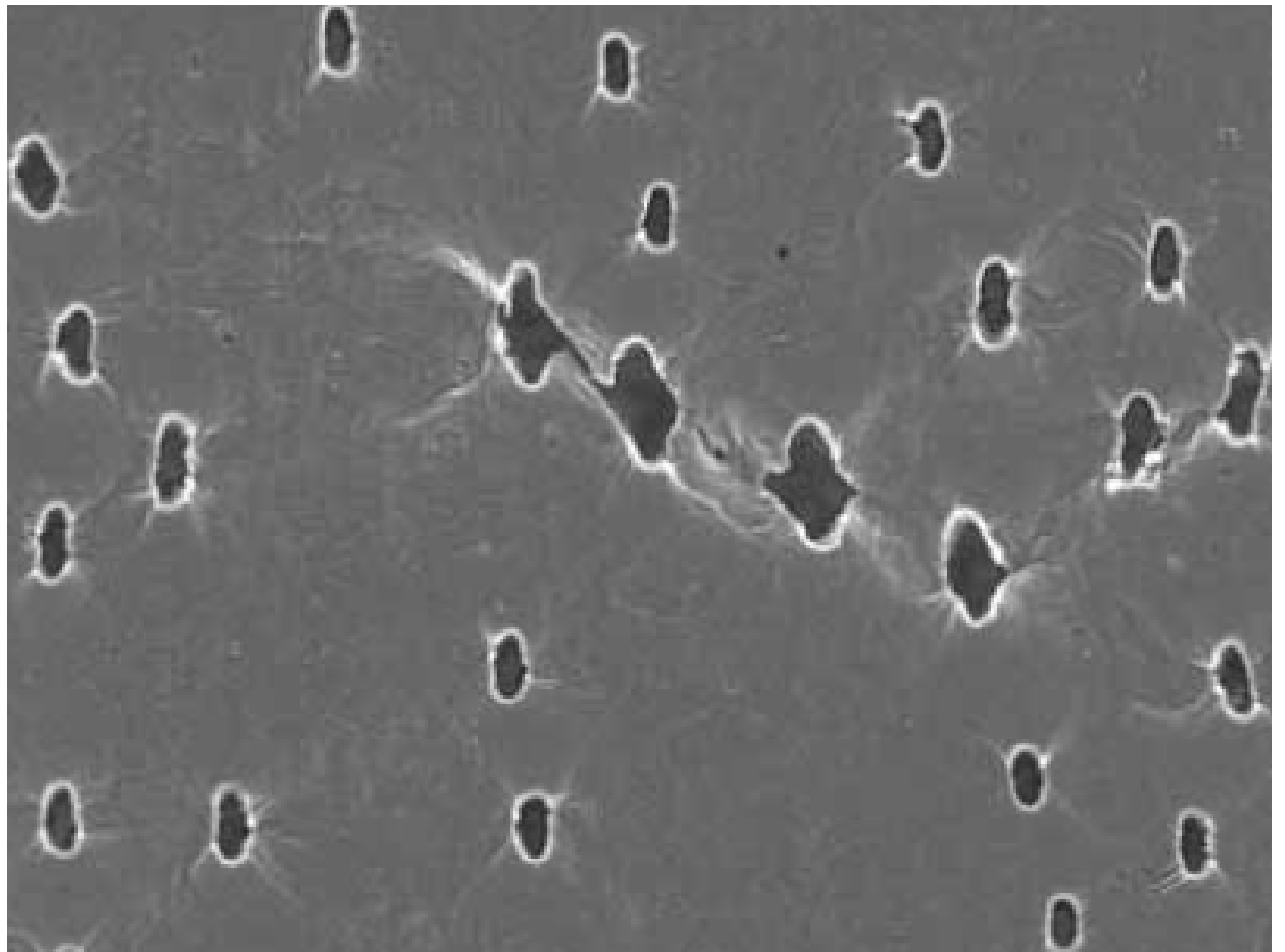
## Deformation sequence of a 2D model material:

- A 100  $\mu\text{m}$  thick metallic (aluminum alloy 5052) sheet
- The diameter of the laser-drilled holes is at least 10  $\mu\text{m}$ .
- The pictures are taken in-situ in a scanning electron microscope (SEM)

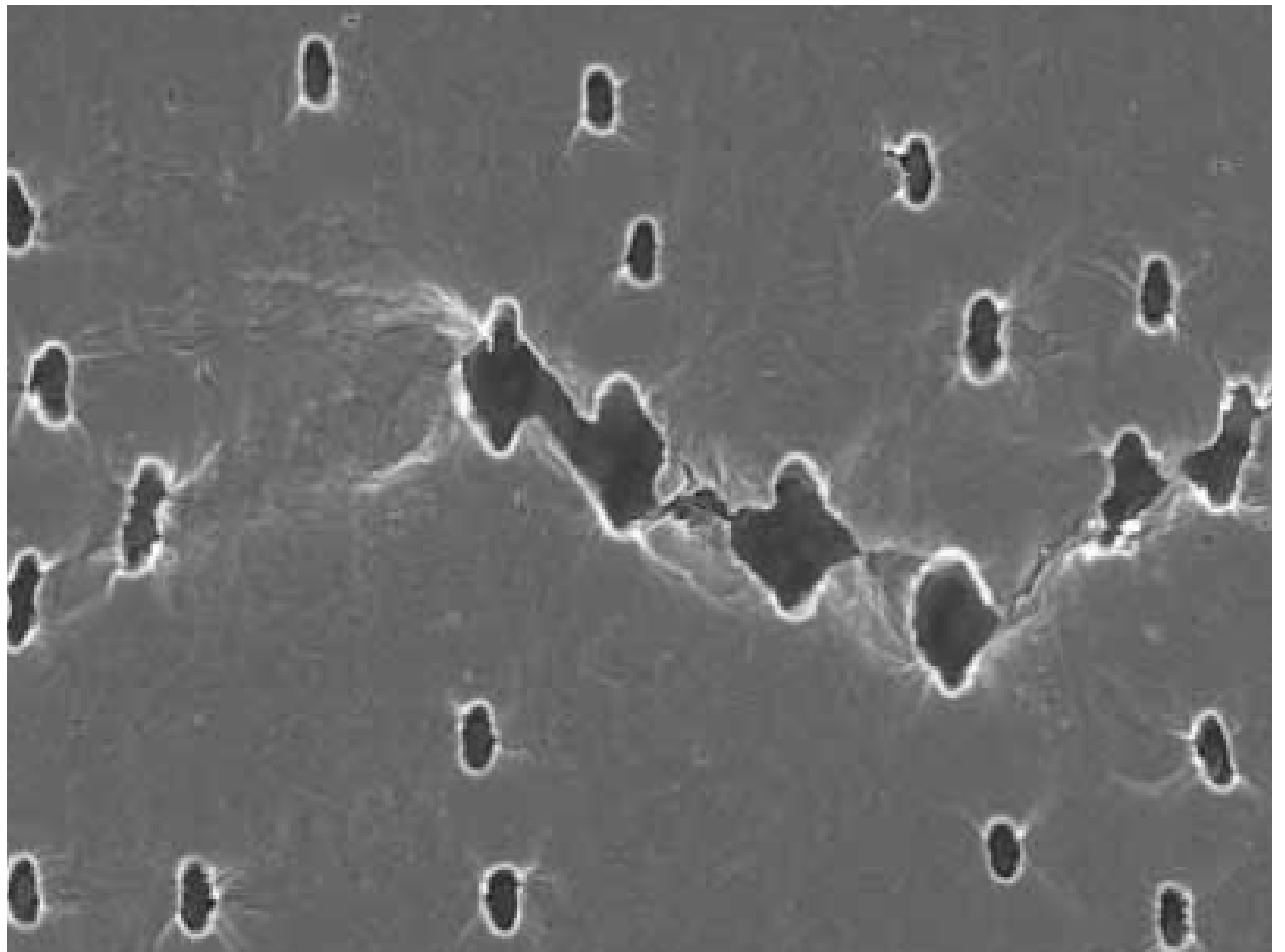






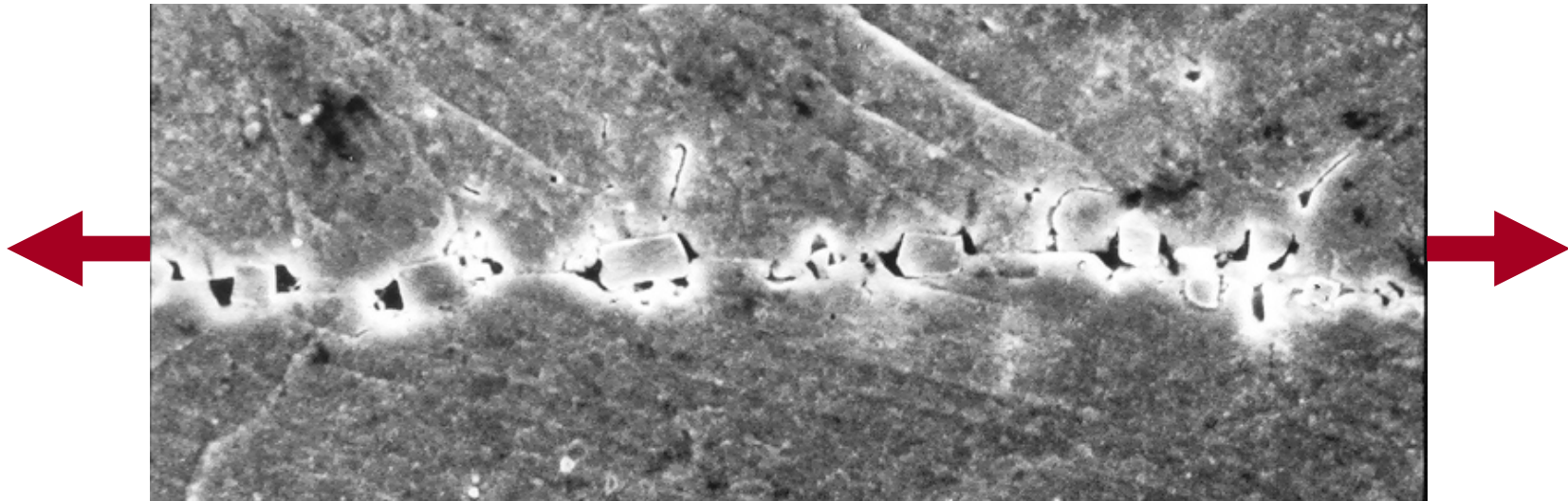








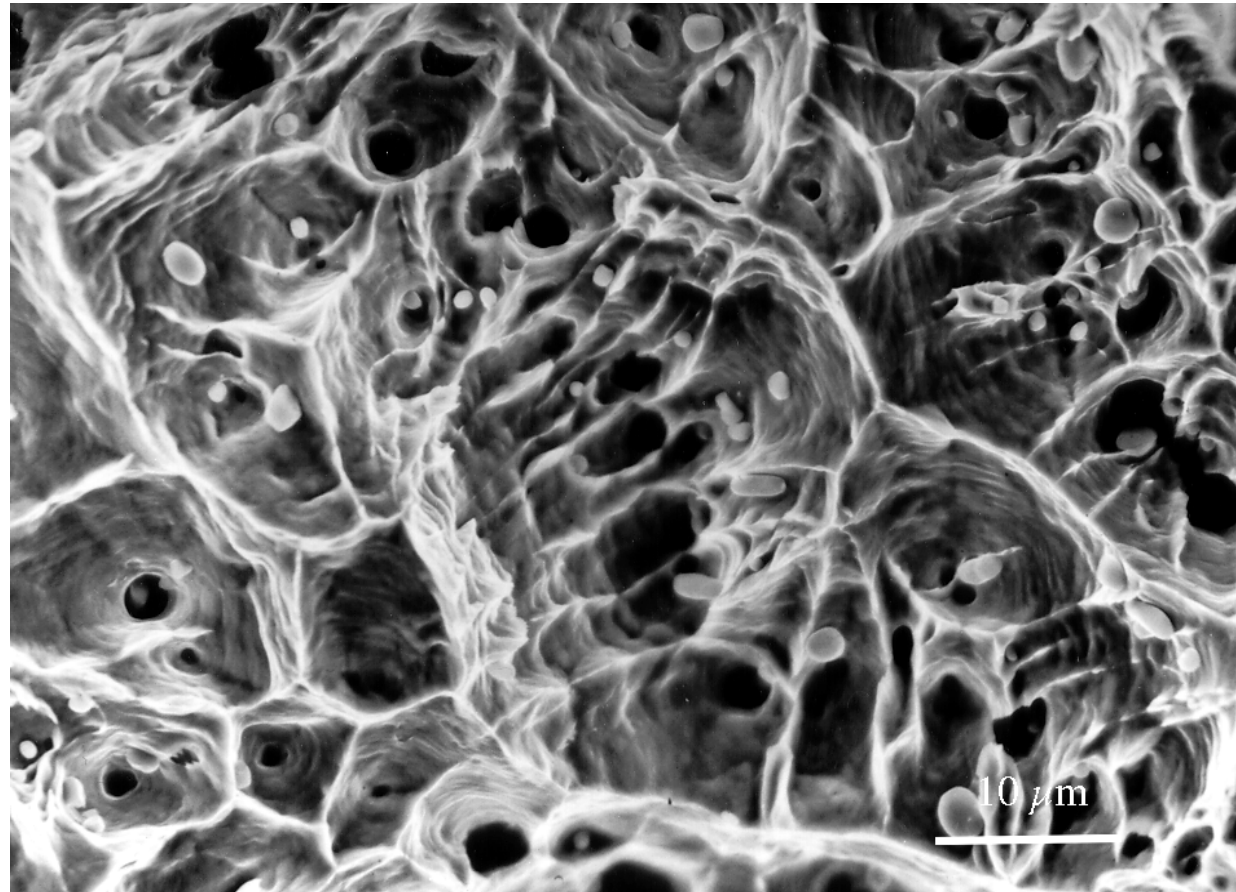
## More anecdotic coalescence mechanism : coalescence in column



Micrograph : *metallographically prepared specimen made of extruded Cu bars, deformed in tension up to large strains (Pardoen, 1998)*



## Final configuration : the fracture surface

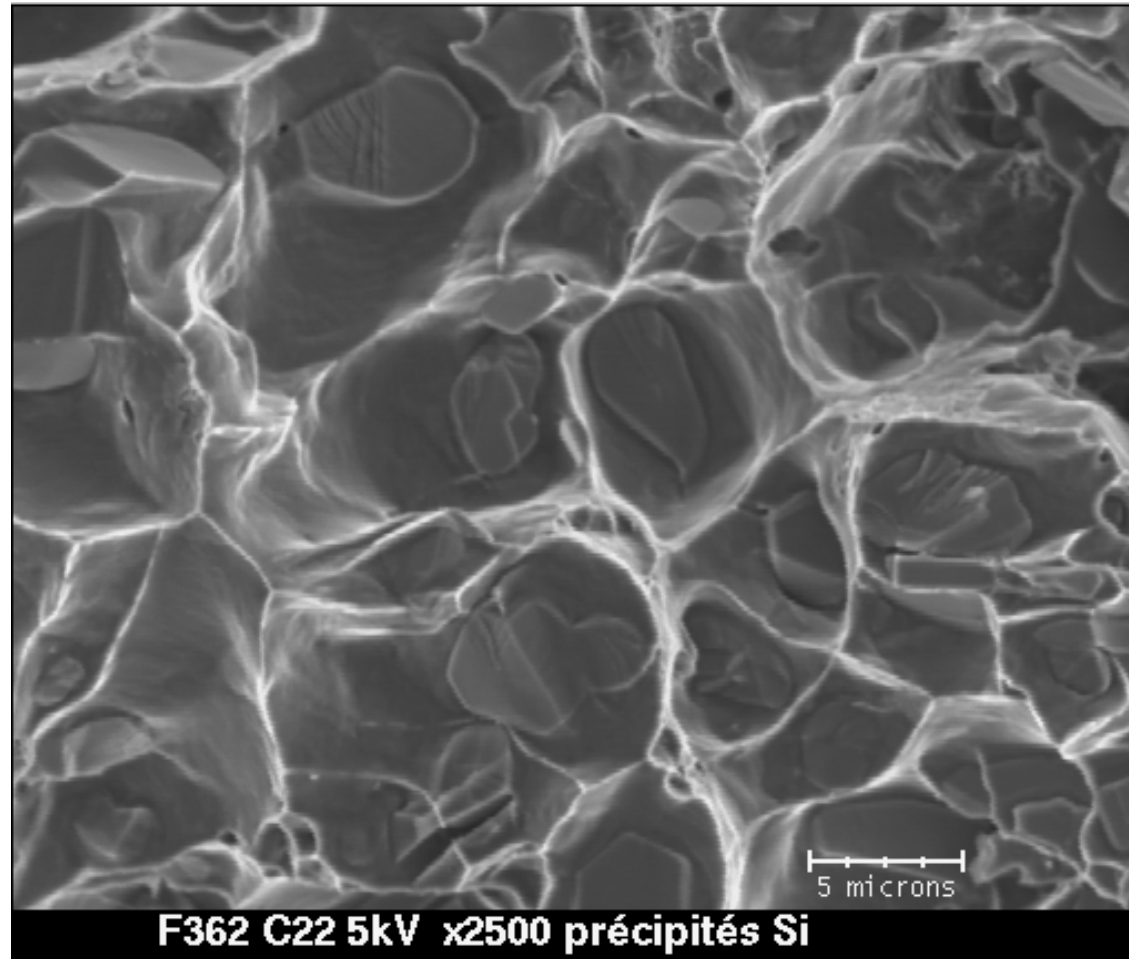


Typical of ductile fracture - here voids have nucleated by decohesion of CuO inclusions inside Cu, see inclusions inside the dimples.



**UCL**

Université  
catholique  
de Louvain

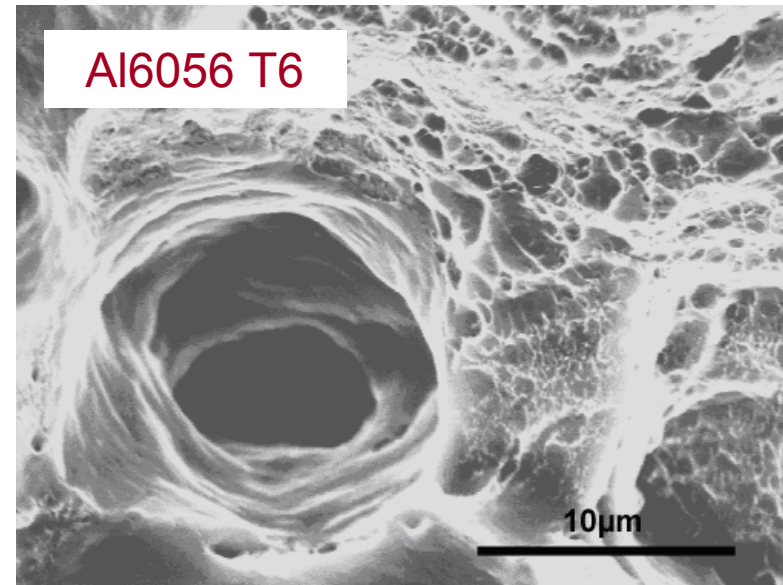
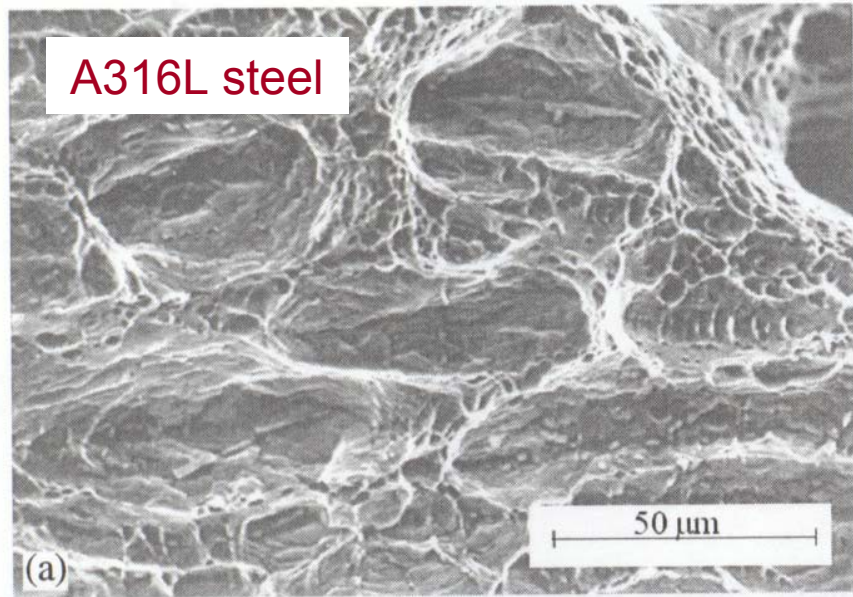


Fracture surface with dimples, typical of ductile fracture (here voids have nucleated by fracture of Si inclusions inside an Al matrix, see broken inclusions inside the dimples)

## Secondary voids are often observed on fracture surfaces of metallic alloys

Second populations of voids result from nucleation on submicron sized particles at large strains, e.g.

- carbides in steel
- dispersoids in Al alloys
- small  $\alpha$  particles in  $\alpha/\beta$  Ti alloys

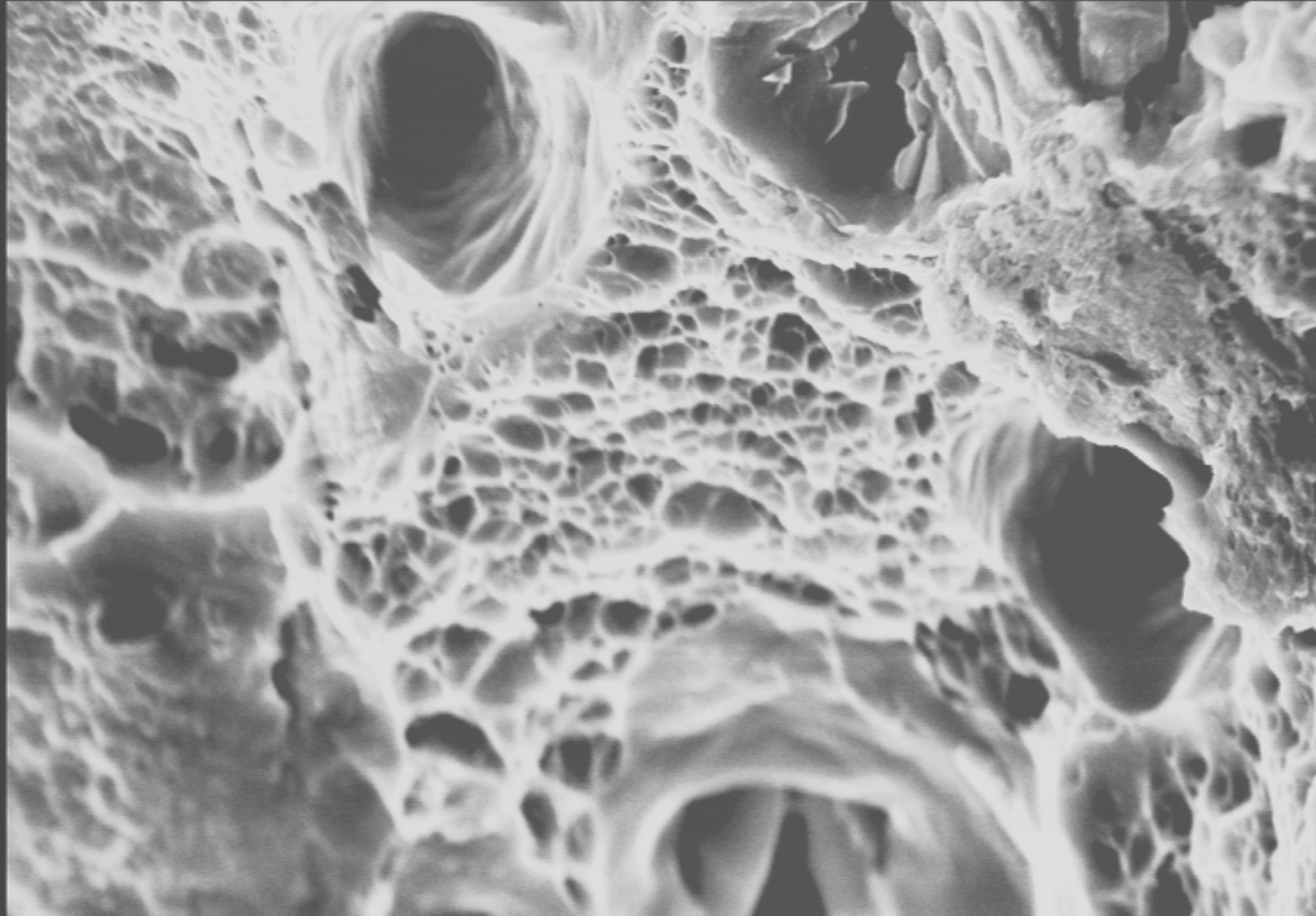




**UCL**

Université  
catholique  
de Louvain

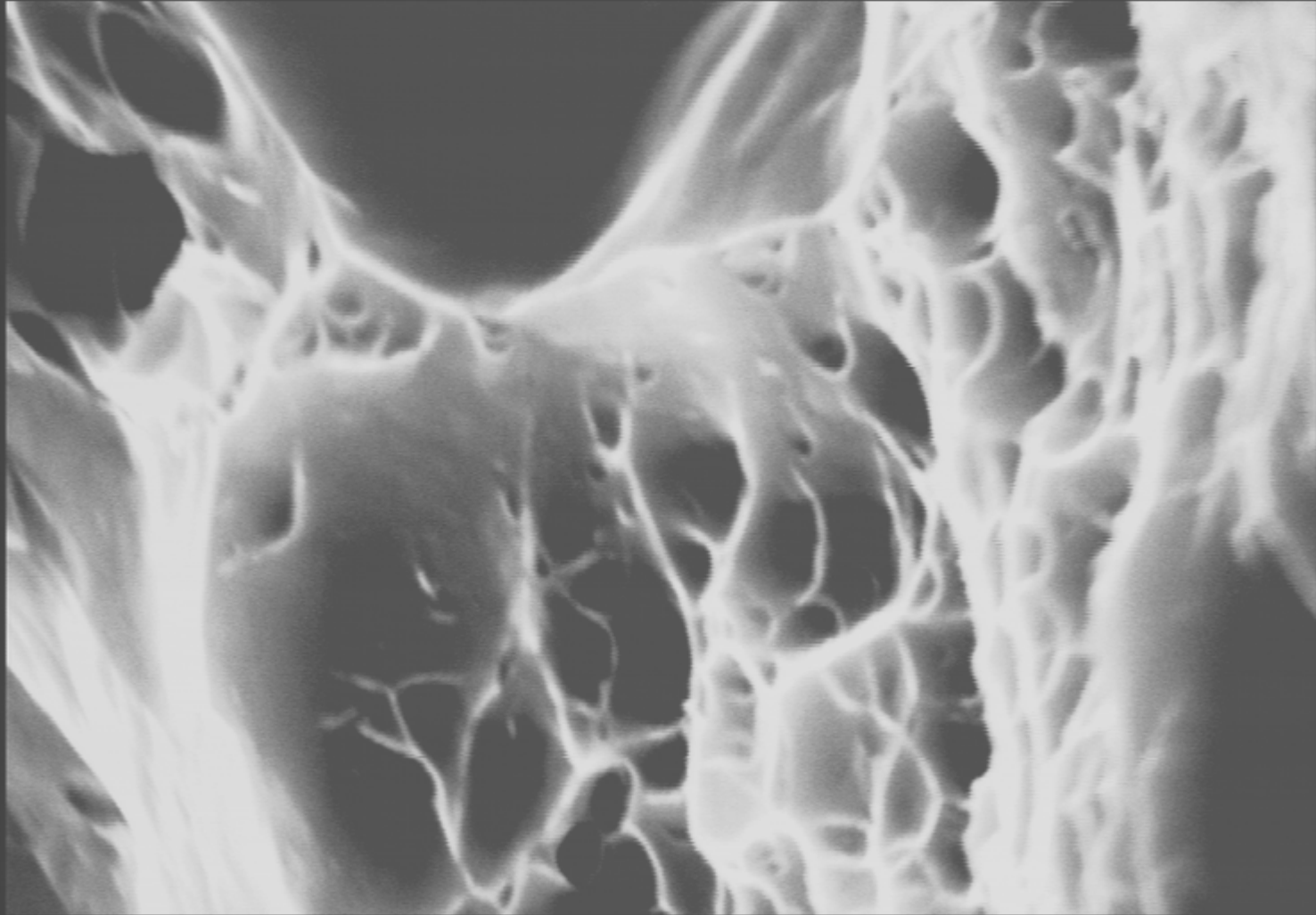
2.50kX 20kV WD:15mm S:00000 P:00000  
20um





**UCL**  
Université  
catholique  
de Louvain

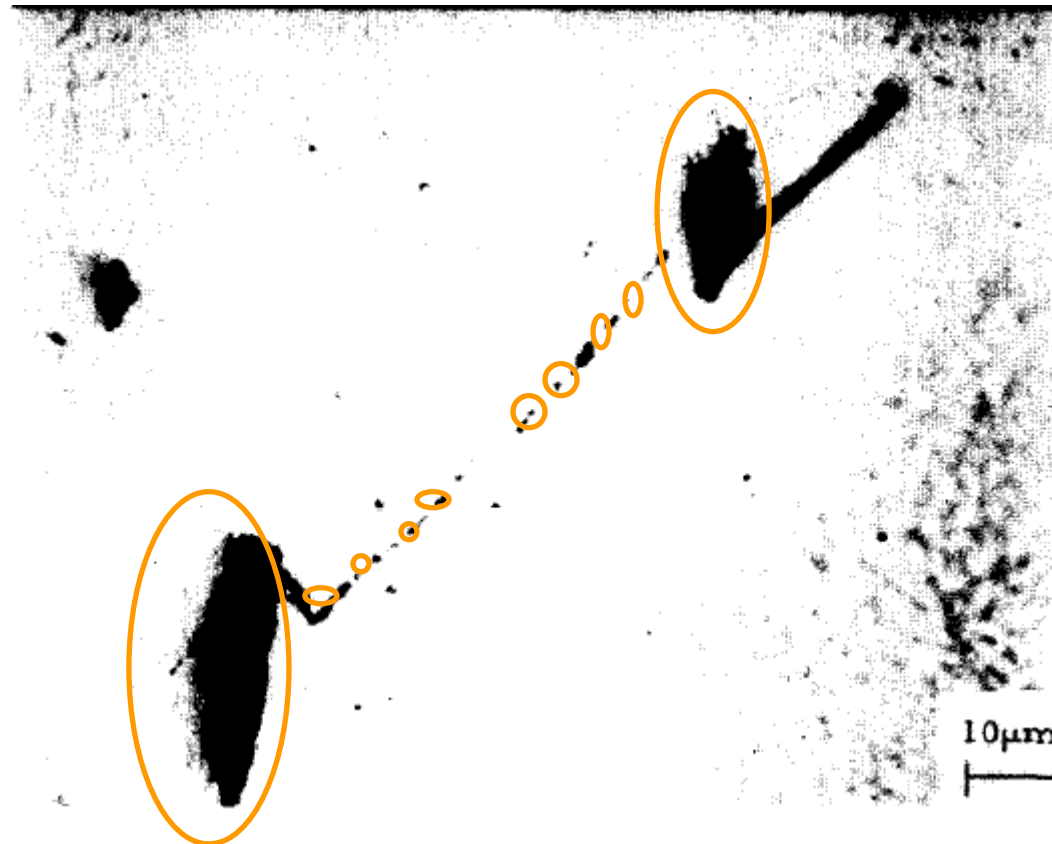
8.88kX 20kV WD:15mm S:00000 P:00000  
5um





**UCL**

Université  
catholique  
de Louvain



Cox, T. B. and Low, J. R., Jr. (1974) An investigation of the plastic fracture of AISI 4340 and 18 Nickel-200 grade maraging steels. *Metallurgical Transactions* **5**, 1457-1470.



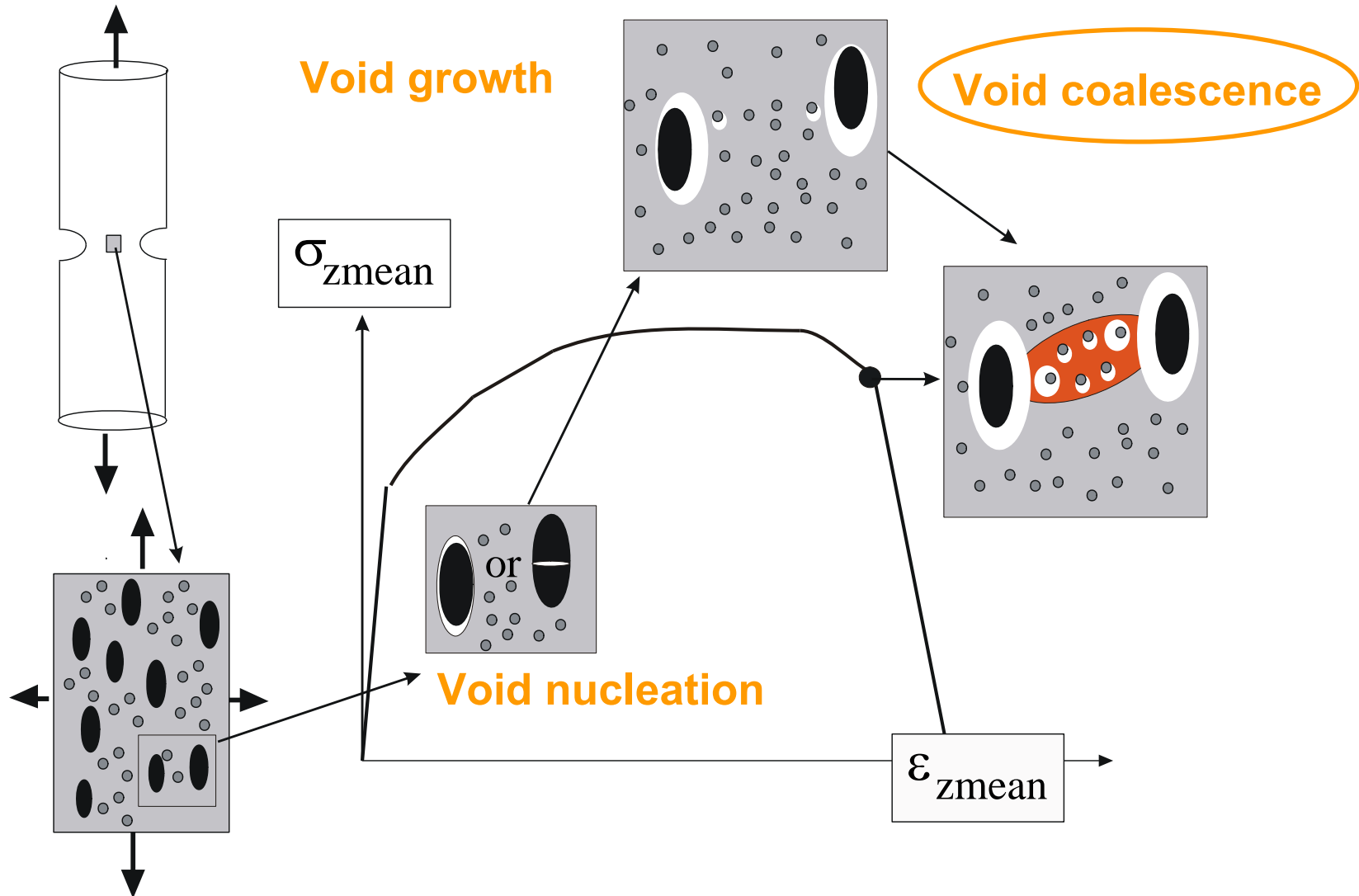
# Summary

- Void coalescence can be seen as a second stage of void growth but with the plastic flow localized in the intervoid ligament
- Void coalescence can take place
  - (1)  $\pm$  normal to the main loading direction « internal necking »
  - (2)  $\pm$  in the direction of maximum shear « coalescence in shear »
  - (3) in columns (... anecdotic)

depending on the void arrangement, loading mode and strain hardening capacity

- Void coalescence can be accelerated by the presence of a second population of voids (in shear : « void sheeting »)
- Distinguish « onset of coalescence » and « coalescence »
- Void coalescence should not be confused with (meso) plastic localization mechanisms resulting from the damage induced softening, involving effects of the structure and boundary conditions

# Summary

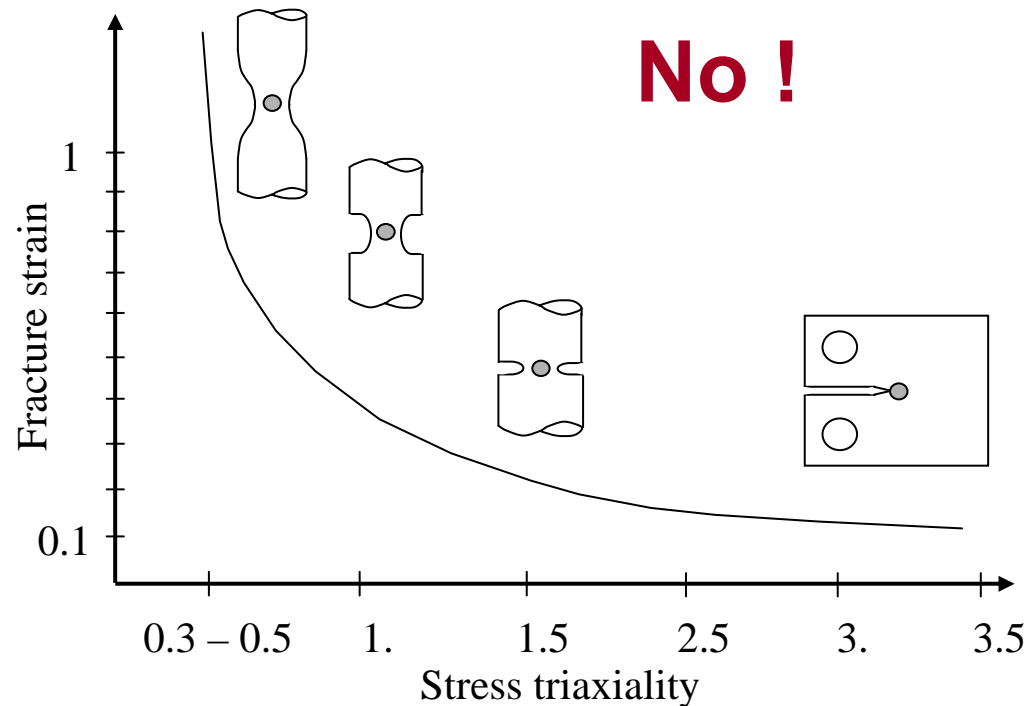


# OUTLINE

1. Experimental observations
2. « Elementary » models for the onset of void coalescence
3. Fine tuning of Thomason model
4. Extension to strain hardening
5. Extension to a second population
6. Extension to combined shear/tension coalescence
7. Models for the coalescence stage

# Empirical models for the onset of void coalescence based on macroscopic quantities

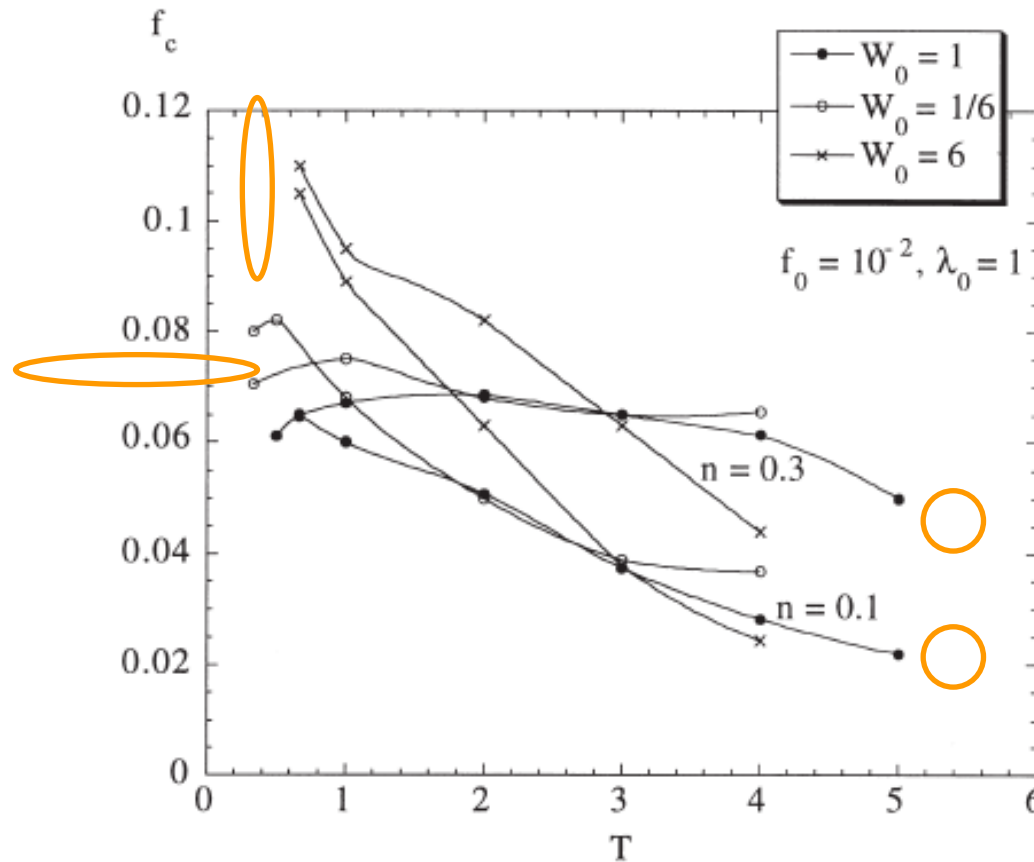
Critical strain ?



Other « critical » combinations of stress and strain (e.g. critical energy density, ...) ? always miss the most important information : **void spacing**

# Critical porosity model

Better, but it does moderately vary with stress triaxiality

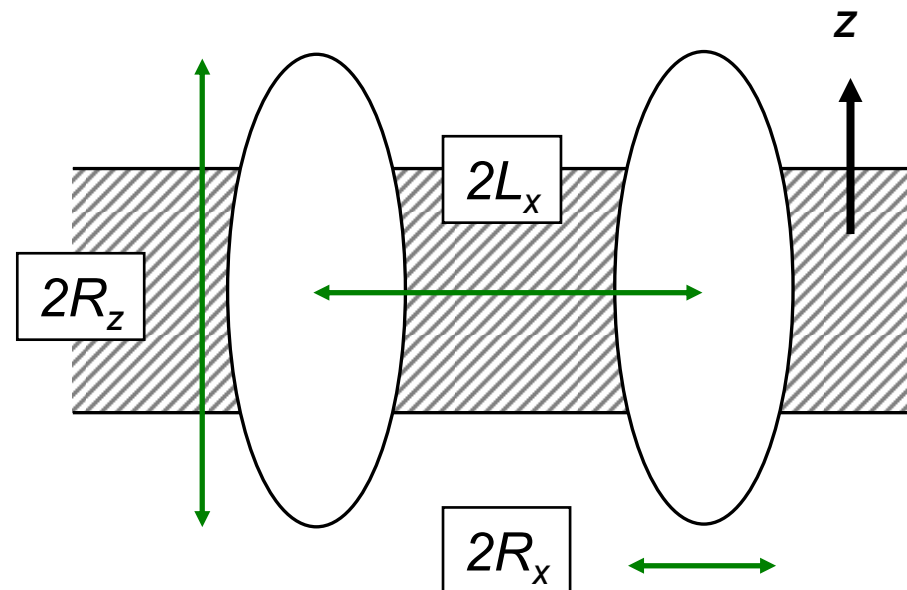


Pardoen & Hutchinson,  
*JMPS* 2000

also misses the most important information : **void spacing**

# Prefer a micromechanical approach for the onset of void coalescence

## Geometry

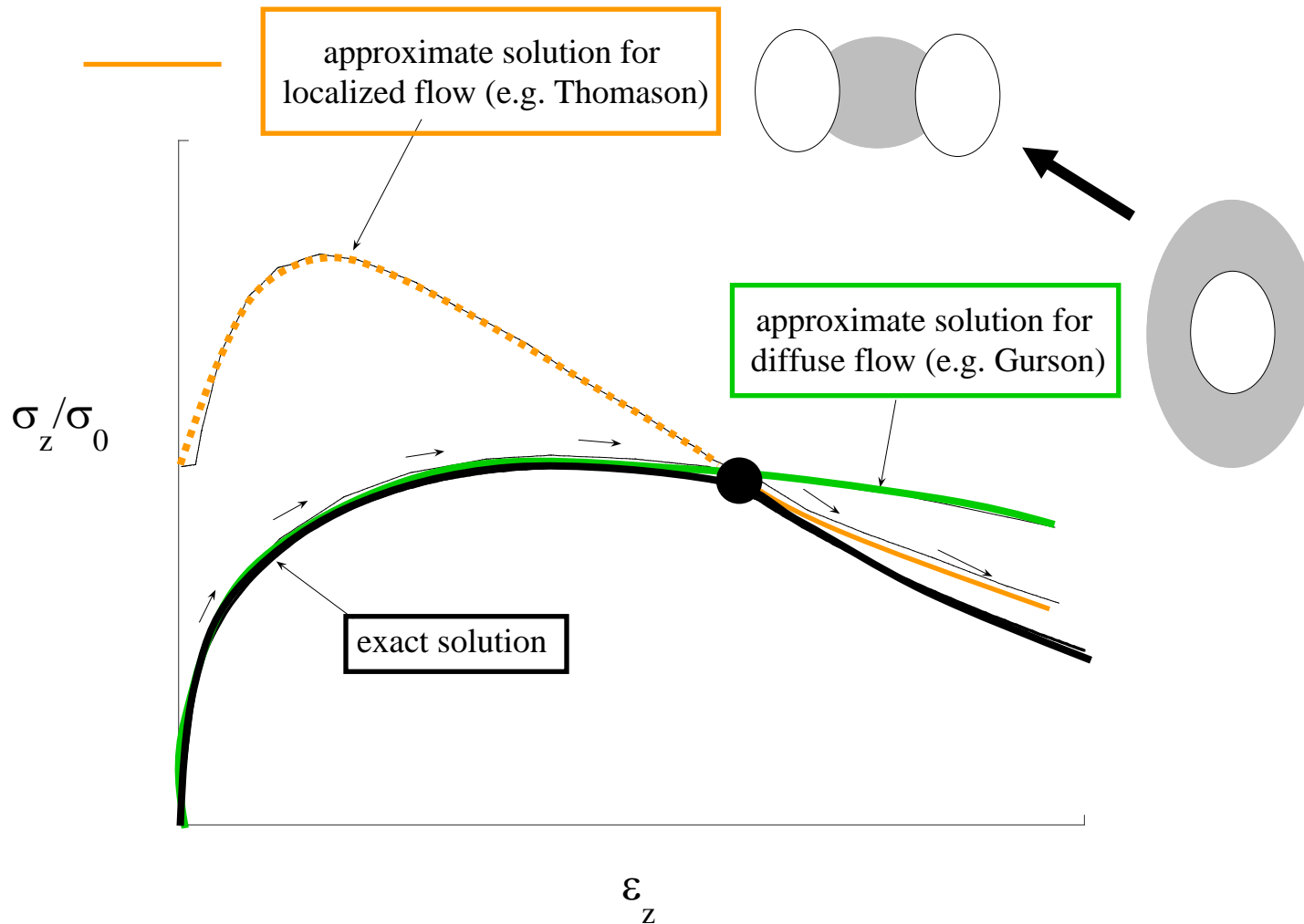


$$\chi = R_x/L_x \text{ (relative void spacing)}$$

$$W = R_z/R_x \text{ (void aspect ratio)}$$

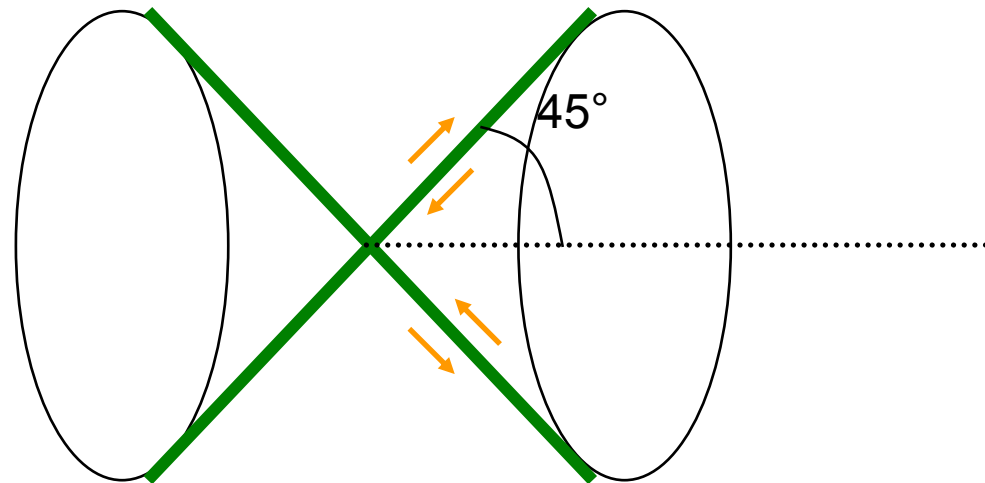
# Construction of a solution for a localized mode of deformation

*Void coalescence : transition to a localized mode of plastic deformation confined in the ligament between neighbouring voids*



## Brown and Embury (1973)

Coalescence (internal necking) sets in when two 45° shear bands can connect the two neighbouring voids



$$\chi \sqrt{1 + W^2} = 1$$

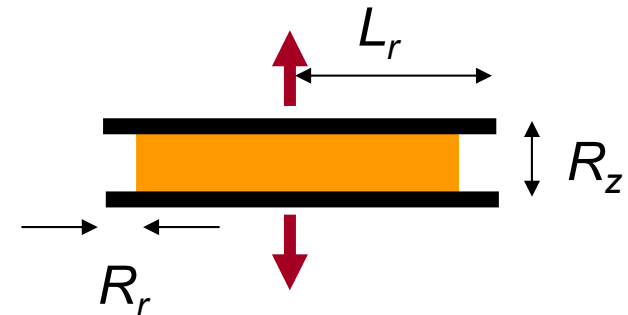


## Hill (1950)

*An approximate analysis for the limit load of this configuration, with associated average true stress, can be carried out along the lines of Hill's (1950) plane strain analysis of a thin plastic layer welded to and squeezed by two rigid platens. The analysis assumes the material in the disk moves outward flowing in shear and otherwise supporting only hydrostatic tension such that the three normal stresses are approximately equal.*

*Radial equilibrium (with the approximation that the normal stresses at the void are zero) provides the applied stress as a function of the current geometry*

$$\frac{\Sigma_z}{\sigma_0} = \frac{2}{3\sqrt{3}} \frac{L_r}{R_z} \left(1 - \frac{R_r}{L_r}\right)^2 \left(2 + \frac{R_r}{L_r}\right)$$

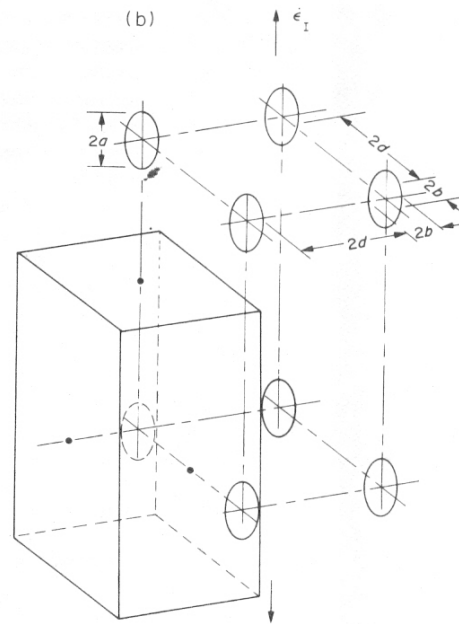
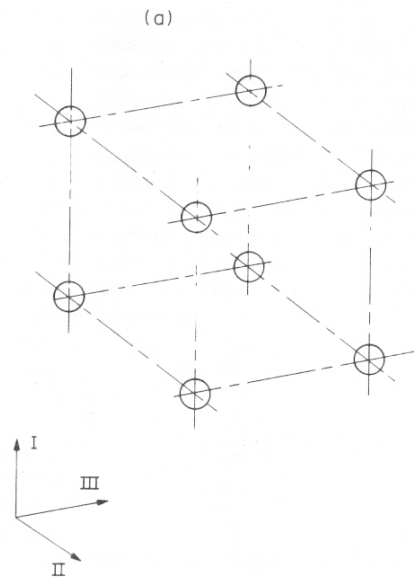


Volume conservation

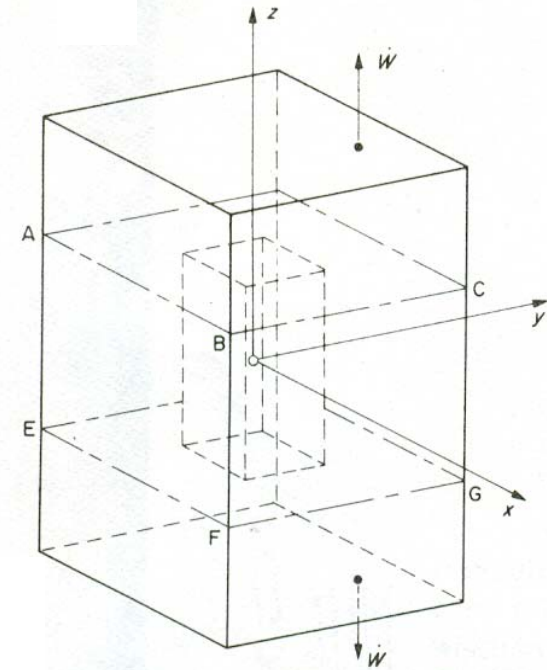
$$\frac{R_z}{R_{z0}} = \frac{1 - (R_{r0} / L_r)^2}{1 - (R_r / L_r)^2}$$

$$E_z = \ln \left[ (R_z - R_{z0}) / L_{z0} \right]$$

# Thomason (1968,1985)



Initial geometry

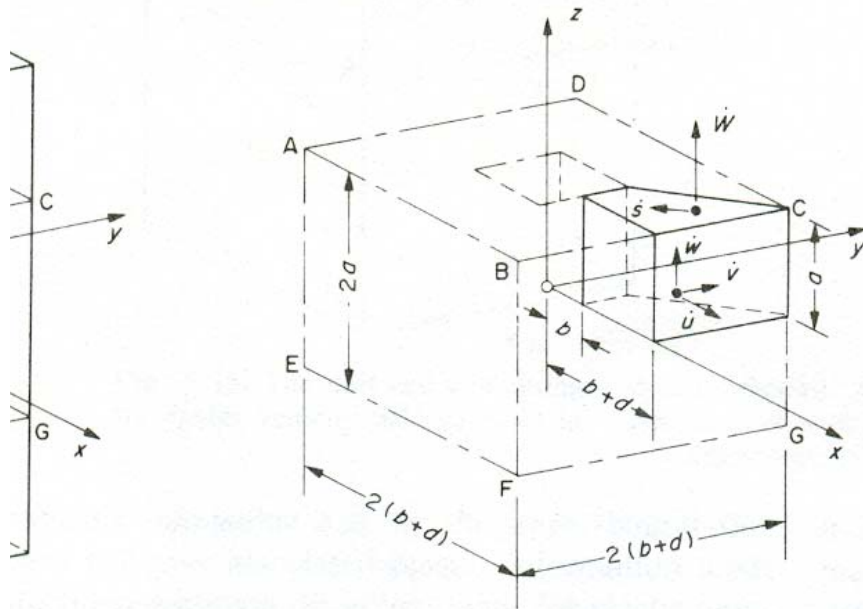


Ellipsoidal voids  
simplified as square  
prismatic voids

# Thomason (1968,1985)

Upper bound analysis – propose kinematically admissible velocity fields

« parallel » velocity field  
(solution 1)

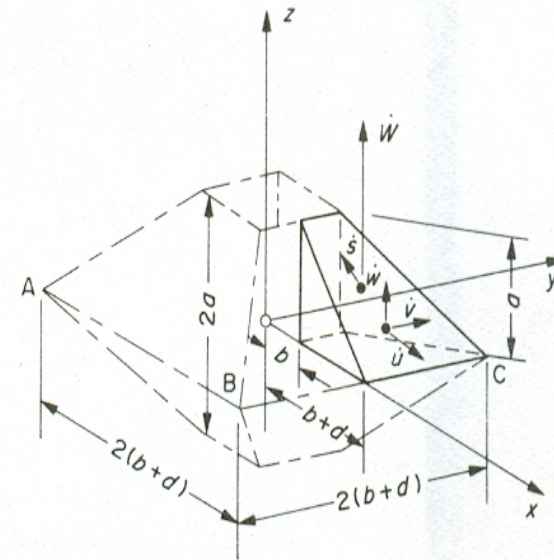


$$\begin{aligned} a &= R_z \\ b &= R_x \\ d &= L_x - R_x \end{aligned}$$

$$\begin{aligned} \dot{u}(x, y, z) &= \frac{\dot{W}}{2R_z x} (L_x^2 - x^2) \\ \dot{v}(x, y, z) &= \frac{\dot{W}}{2R_z x^2} (L_x^2 - x^2) \\ \dot{w}(x, y, z) &= \frac{\dot{W}_z}{R_z} \end{aligned}$$

+ associated tangent velocity discontinuity  $\dot{s}$  at rigid/plastic boundary (see Thomason 1985)

« triangular » velocity field  
(solution 2)



$$\begin{aligned} \dot{u}(x, y, z) &= \frac{\dot{W}(L_x - R_x)}{2R_z x} (L_x + x) \\ \dot{v}(x, y, z) &= \frac{\dot{W}(L_x - R_x)y}{2R_z x^2} (L_x + x) \\ \dot{w}(x, y, z) &= -\frac{\dot{W}_z(L_x - R_x)}{2R_z x} \end{aligned}$$

## Thomason (1968,1985)

Rate of internal work

$$\dot{I} = \sqrt{\frac{2}{3}} \sigma_0 \int_V \sqrt{\dot{\varepsilon}_{xx}^2 + \dot{\varepsilon}_{yy}^2 + \dot{\varepsilon}_{zz}^2 + \frac{1}{2} (\dot{\varepsilon}_{xy}^2 + \dot{\varepsilon}_{yz}^2 + \dot{\varepsilon}_{xz}^2)} dV + \frac{\sigma_0}{\sqrt{3}} \int_S \dot{s} dS$$

=

Rate of external work

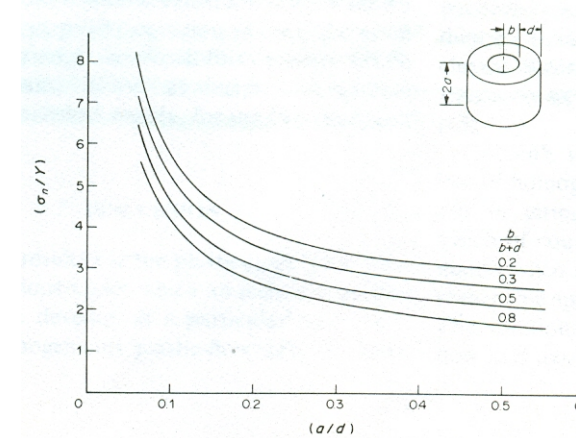
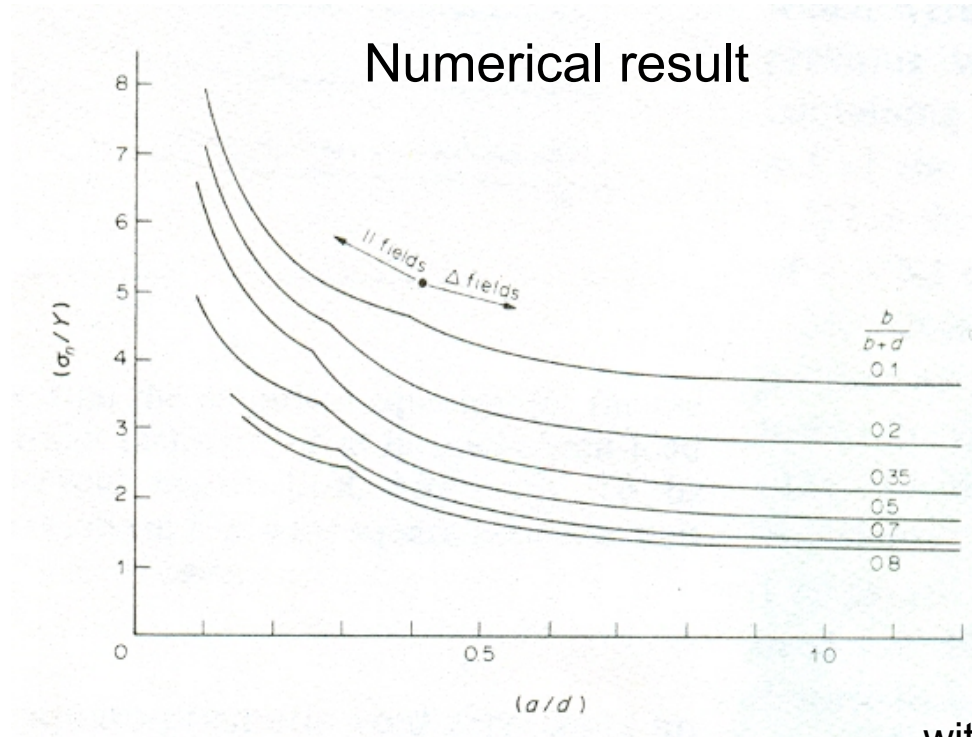
$$\dot{E} = \sigma_n A_n \dot{W}$$

with  $\sigma_n$  applied on the  
non porous (effective)  
surface

using 
$$\dot{\varepsilon}_{ij} = \frac{1}{2} \left( \frac{\partial \dot{u}_i}{\partial x_j} + \frac{\partial \dot{u}_j}{\partial x_i} \right)$$

and  $u_1 = u, u_2 = v, u_3 = w$

# Thomason (1968,1985)



Note : ressemble  
cylindrical solution

with  $\eta$  a function of void distribution

$$\frac{\sigma_n}{\sigma_0} = \left[ 0.1 \left( \frac{1-\chi}{\chi W} \right)^2 + 1.2 \sqrt{\frac{1}{\chi}} \right]$$

$$\frac{\sigma_z}{\sigma_0} = (1-\eta\chi^2) \left[ 0.1 \left( \frac{1-\chi}{\chi W} \right)^2 + 1.2 \sqrt{\frac{1}{\chi}} \right]$$

$\chi$  is the key parameter



Note the extension by Benzerga, Besson, Pineau (2000)

$$\frac{\Sigma_{22}}{\sigma_0} = (1 - \eta\chi^2) \left[ \alpha \left( \frac{\chi^{-1} - 1}{W^2 + 0.1\chi^{-1} + 0.02\chi^{-2}} \right)^2 + \beta \frac{1}{\sqrt{\chi}} \right]$$



# OUTLINE

1. Experimental observations
2. « Elementary » models for the onset of void coalescence
3. Fine tuning of Thomason model (**perfect plasticity**)
4. Extension to strain hardening
5. Extension to a second population
6. Extension to combined shear/tension coalescence
7. Models for the coalescence stage



**UCL**  
Université  
catholique  
de Louvain



Contents lists available at SciVerse ScienceDirect

**Journal of the Mechanics and Physics of Solids**

journal homepage: [www.elsevier.com/locate/jmps](http://www.elsevier.com/locate/jmps)



## A criterion for the onset of void coalescence under combined tension and shear

C. Tekoğlu<sup>a,\*</sup>, J.-B. Leblond<sup>b</sup>, T. Pardoen<sup>c</sup>

<sup>a</sup> Department of Mechanical Engineering, TOBB University of Economics and Technology, Söğütözü, Ankara 06560, Turkey

<sup>b</sup> Institut Jean-Le-Rond-d'Alembert, Université Paris VI, Tour 65-55, 4, Place Jussieu, 75252 Paris Cedex 05, France

<sup>c</sup> Institute of Mechanics, Materials and Civil Engineering, Université catholique de Louvain, Place Sainte Barbe 2, B-1348 Louvain-la-Neuve, Belgium

### ARTICLE INFO

#### Article history:

Received 24 June 2011

Received in revised form

23 January 2012

Accepted 19 February 2012

Available online 24 February 2012

#### Keywords:

Ductility

Fracture mechanisms

Voids and inclusions

Finite elements

Limit-load analysis

### ABSTRACT

Depending on the relative positions of voids and on the loading conditions, shear loading components can play an important role in the void coalescence process leading to ductile fracture. Yet, most void coalescence criteria including the original criterion of Thomason, and its various extensions/improvements, take only normal loads into account and neglect the contribution from shear loads to coalescence. Shear can affect both the stress/strain at the onset of coalescence and the direction of deformation localization. In this paper, first, the predictive capabilities of different coalescence criteria without shear effect are critically assessed and the expressions involved in the original Thomason criterion are fine-tuned by comparing with 3D finite element calculations performed on a unit cell containing a spheroidal void. Then, the improved Thomason criterion is theoretically extended—by using limit load analysis—to incorporate the effect of shear. The predictions of this new coalescence criterion are in good agreement with the results produced by 3D finite element calculations, for both loadings involving or not a shear component.

© 2012 Elsevier Ltd. All rights reserved.





# Limit Load Analysis with FE Calculations

Elastic perfectly plastic material

$$\frac{E}{\sigma_0} = 444:5; \nu = 0:49$$

Predominant axial stress state

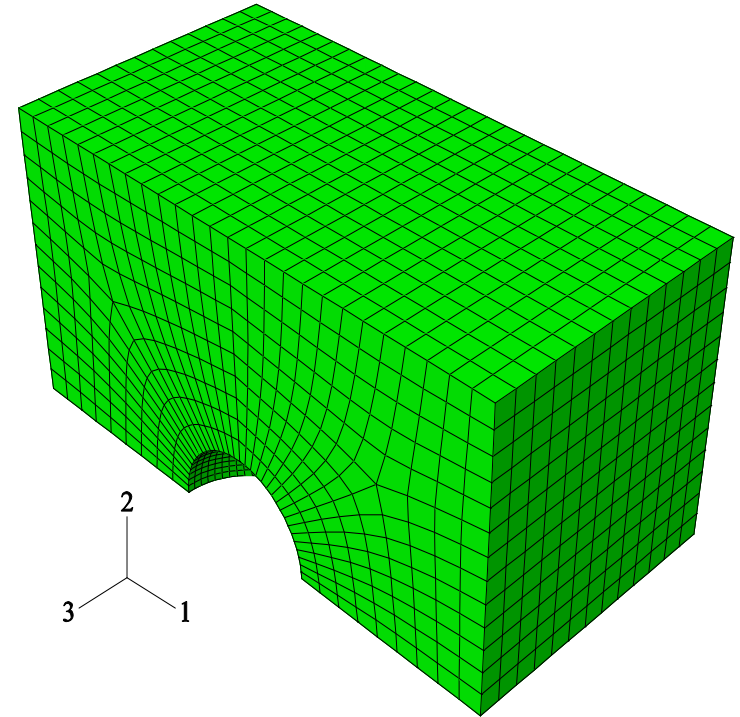
$$\Sigma_{22} > \Sigma_{11} (= \Sigma_{33})$$

Displacement BC's are applied

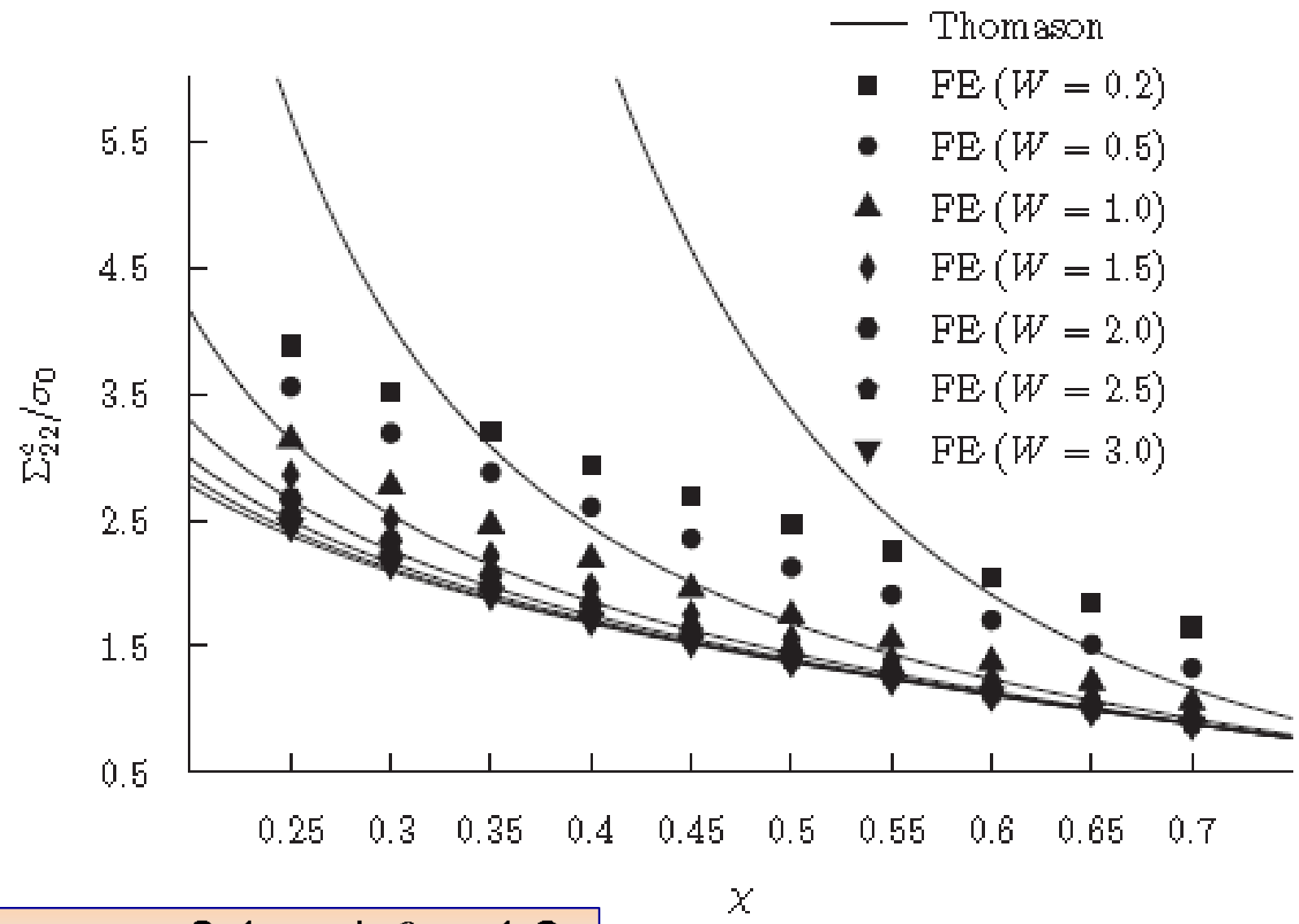
$$E_{22} > E_{11} (= E_{33})$$

Equilibrium eqs. are solved on the initial configuration

$$W = W_0 \text{ and } A = A_0$$

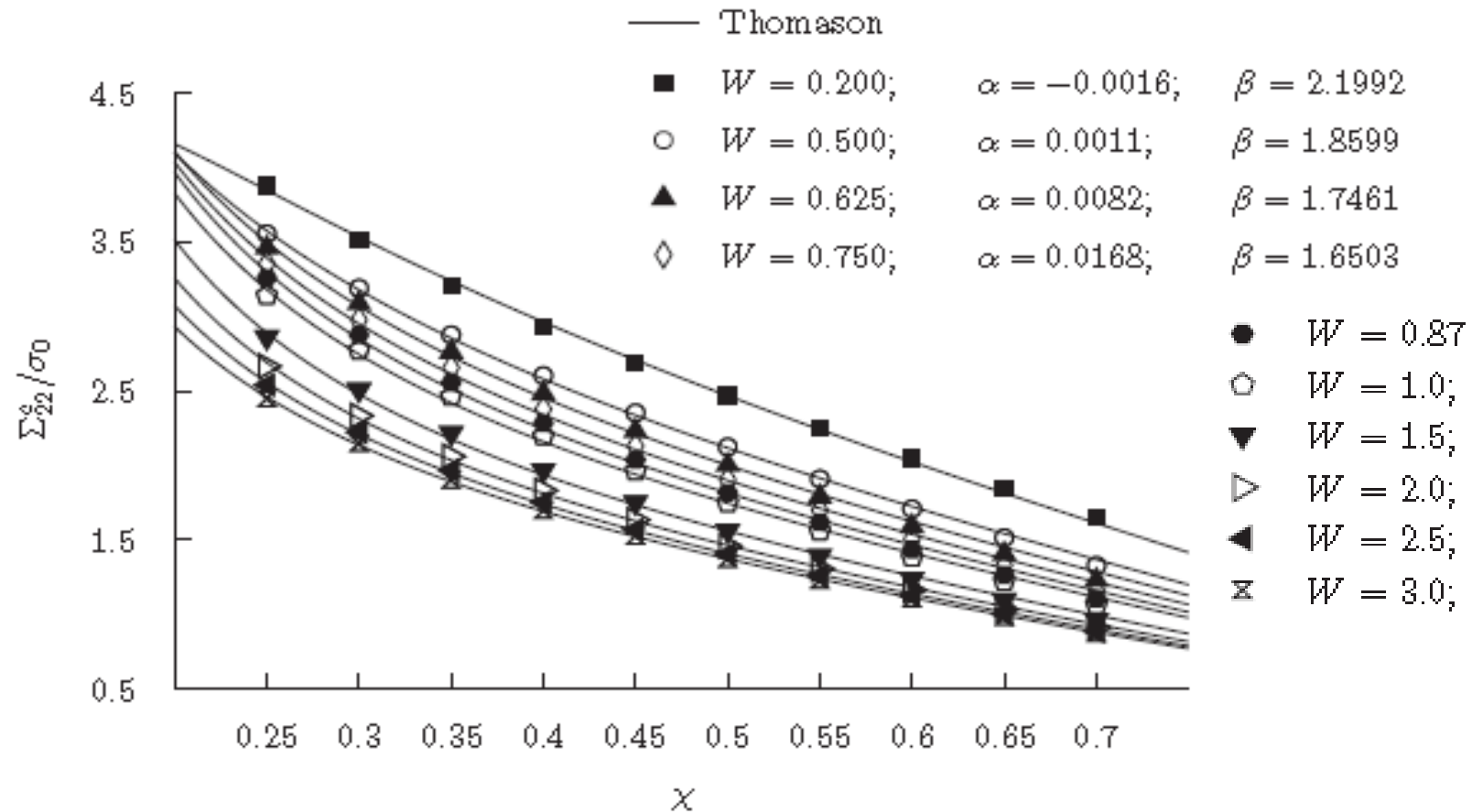


# Onset of coalescence (Thomason versus FE)



with  $\alpha = 0.1$  and  $\beta = 1.2$

# Modified Thomason versus FE



$$\frac{\Sigma_{22}}{\sigma_0} = (1 - \eta\chi^2) \left[ \alpha^{Th}(W) \left( \frac{1 - \chi}{W\chi} \right)^2 + \beta^{Th}(W) \frac{1}{\sqrt{\chi}} \right],$$

$$\alpha^{Th}(W) = 0.0819W - 0.0373, \quad \beta^{Th}(W) = 0.0036W^5 - 0.0030W^4 - 0.1694W^3 + 0.8499W^2 - 1.6743W + 2.5022$$

# Modified Thomason versus FE

**This is a very recent contribution which was thus, unfortunately, not used in the other enhancements described hereafter.**

# OUTLINE

1. Experimental observations
2. « Elementary » models for the onset of void coalescence
3. Fine tuning of Thomason model
- 4. Extension to strain hardening**
5. Extension to a second population
6. Extension to combined shear/tension coalescence
7. Models for the coalescence stage

## Incorporate strain hardening

$$\frac{\sigma_z}{\sigma_y} = (1 - \eta \chi^2) \left[ 0.1 \left( \frac{1 - \chi}{\chi W} \right)^2 + 1.2 \sqrt{\frac{1}{\chi}} \right]$$

?

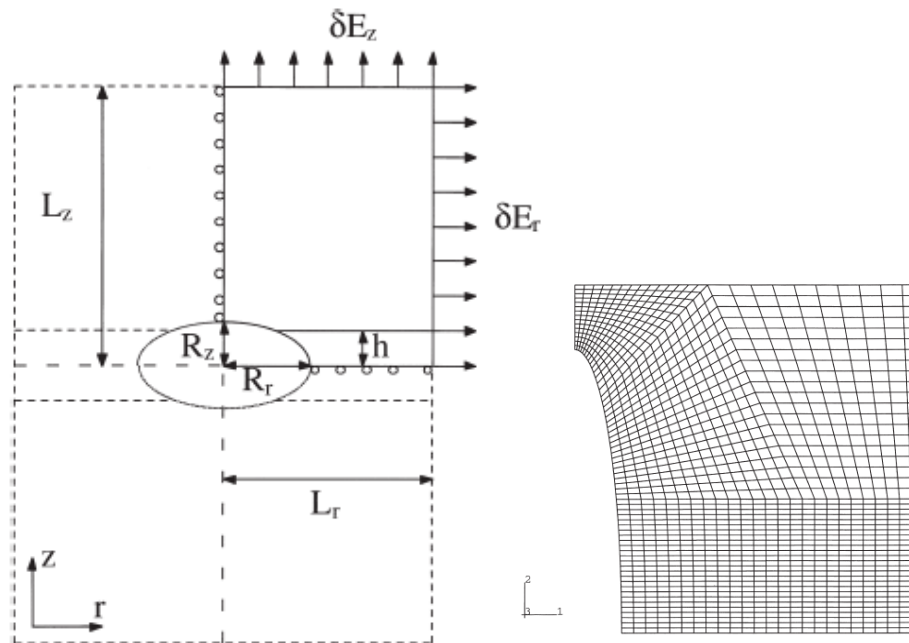
### First approach (2000)

$\sigma_y$  is defined as the average yield stress of the matrix material and computed using the energy balance (Gurson, 1977)

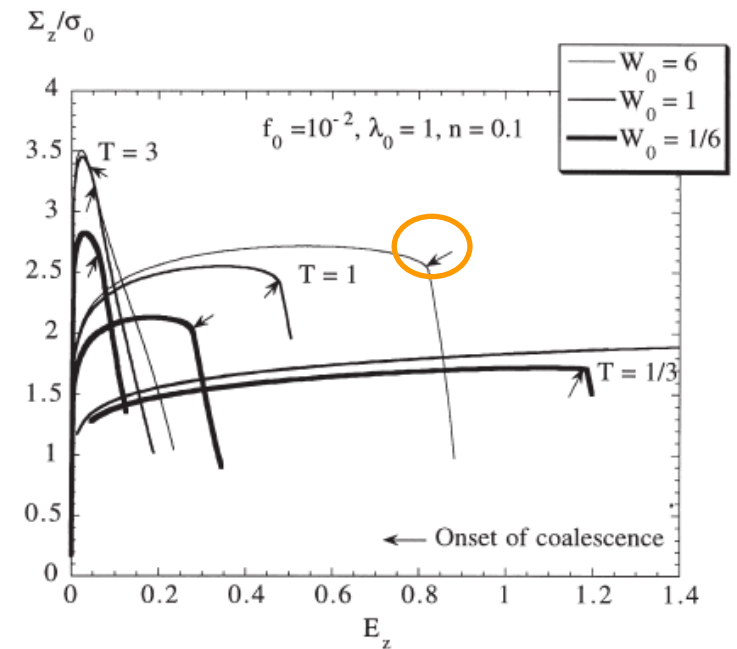
$$\sigma_y \dot{\epsilon}_y^p (1 - f) = \sigma_{ij} \dot{\epsilon}_{ij}^p$$

# Validation of first approach

a. run FE void cell calculations



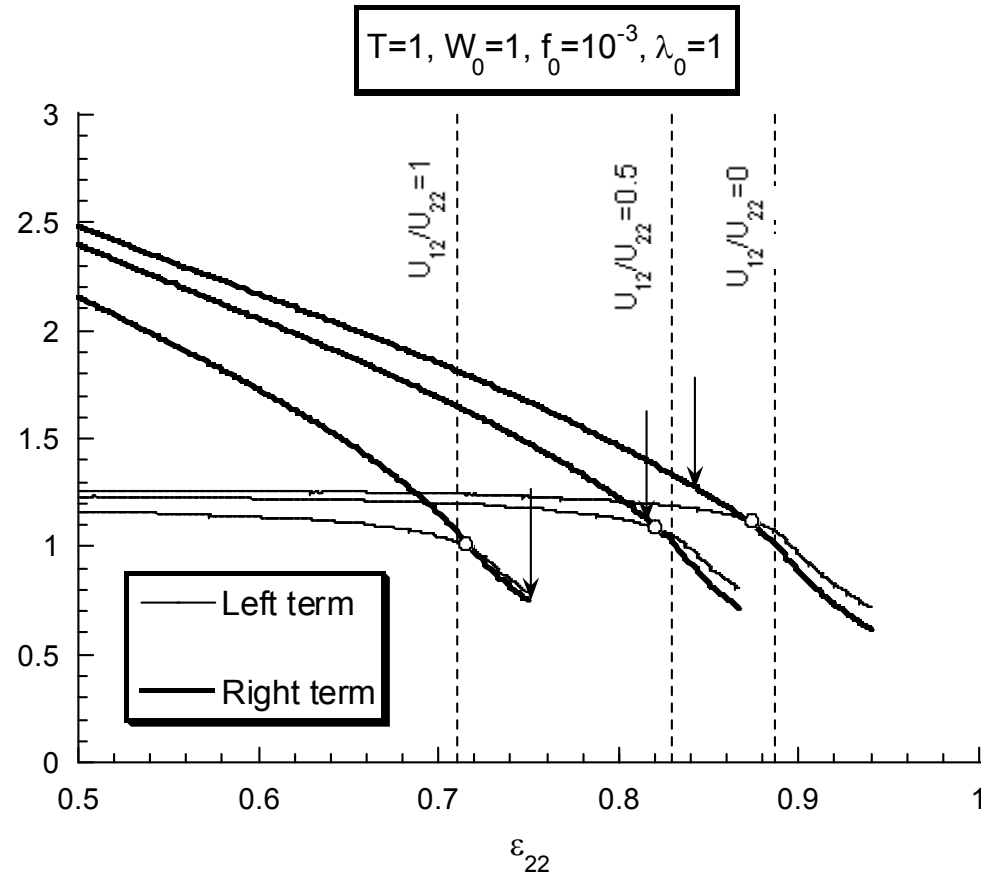
$$\frac{\sigma_z}{\sigma_y} = (1 - \eta \chi^2) \left[ 0.1 \left( \frac{1 - \chi}{\chi W} \right)^2 + 1.2 \sqrt{\frac{1}{\chi}} \right]$$



b. extract from the cell calculation the evolution of  $W$ ,  $\chi$ ,  $\sigma_z$  and  $\sigma_y$

Plug the values into the Thomason model and detect when the criterion is fulfilled

$$\frac{\sigma_z}{\sigma_y} = (1 - \eta\chi^2) \left[ 0.1 \left( \frac{1 - \chi}{\chi W} \right)^2 + 1.2 \sqrt{\frac{1}{\chi}} \right]$$



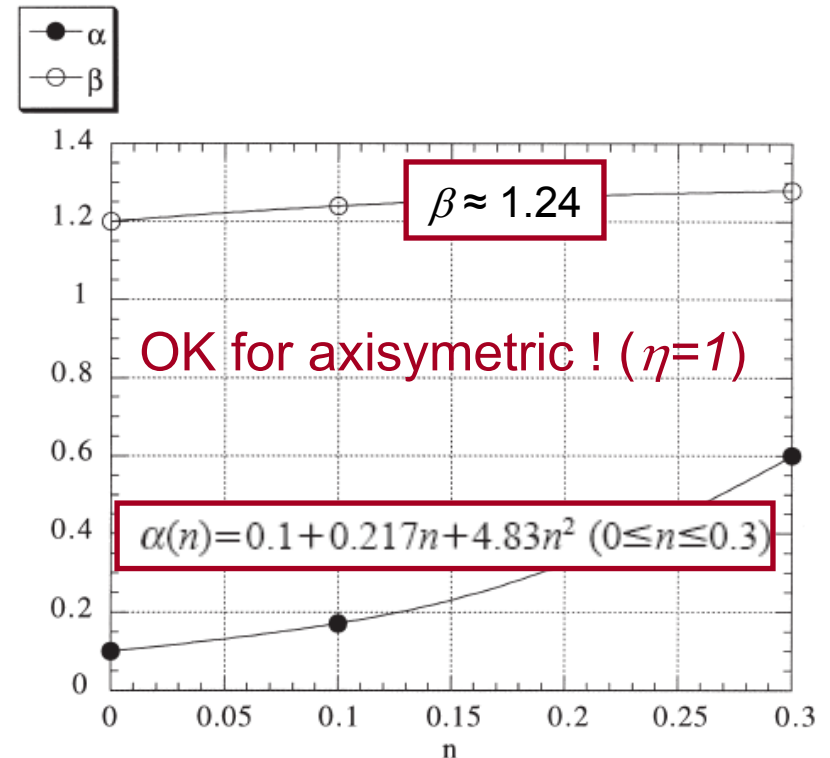
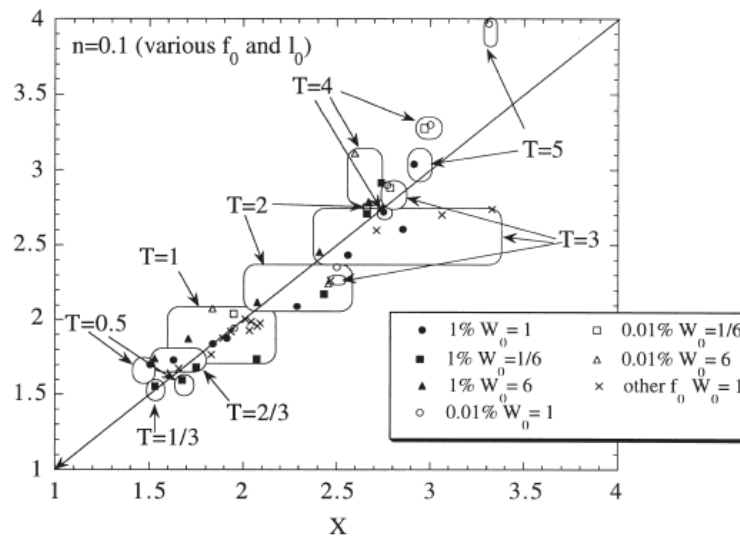


## Result : a strain hardening dependent parameter is required to allow accurate predictions

$$\frac{\sigma_z}{\sigma_y} = (1 - \eta\chi^2) \left[ \alpha(n) \left( \frac{1 - \chi}{\chi W} \right)^2 + \beta(n) \sqrt{\frac{1}{\chi}} \right]$$

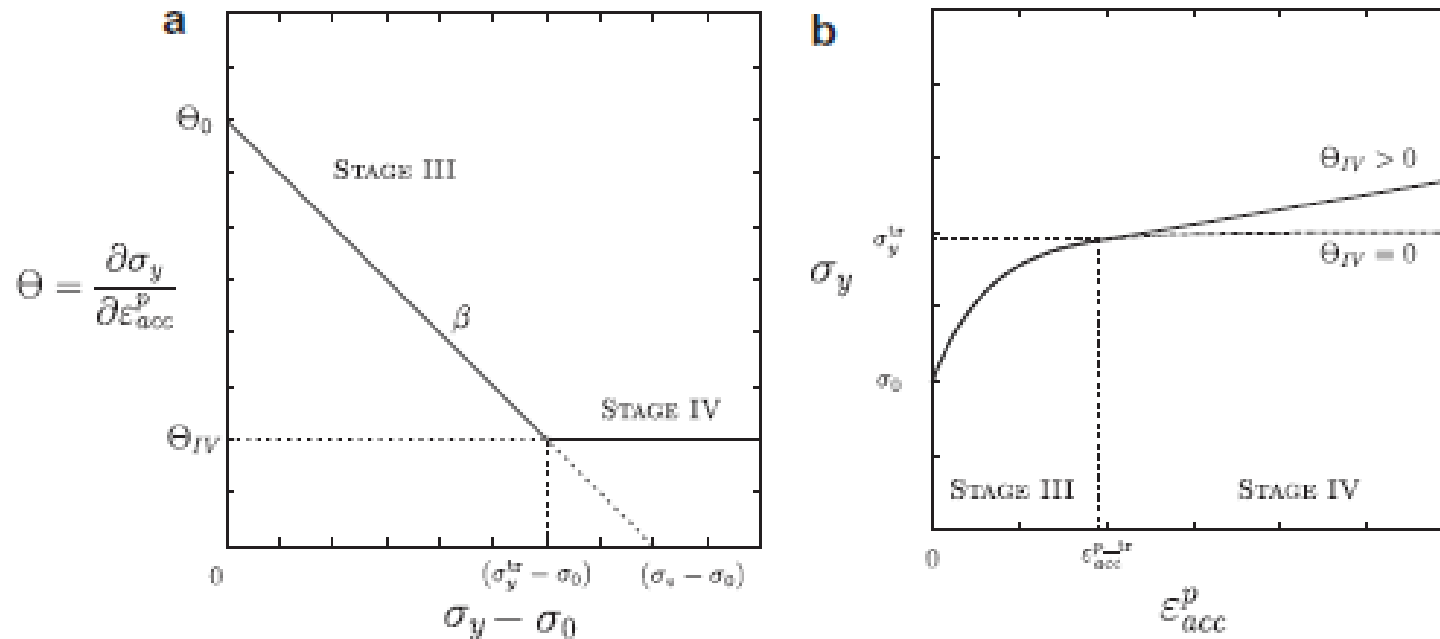
$$\sigma_y = \sigma_0 \left( 1 + \frac{\epsilon_y^p}{\epsilon_0} \right)^n$$

Y ( $\alpha=0.17$   $\beta=1.24$ )



But, not elegant + what do we do when power law  
hardening does not apply?

## What if a more physical hardening Voce law with stage IV ?

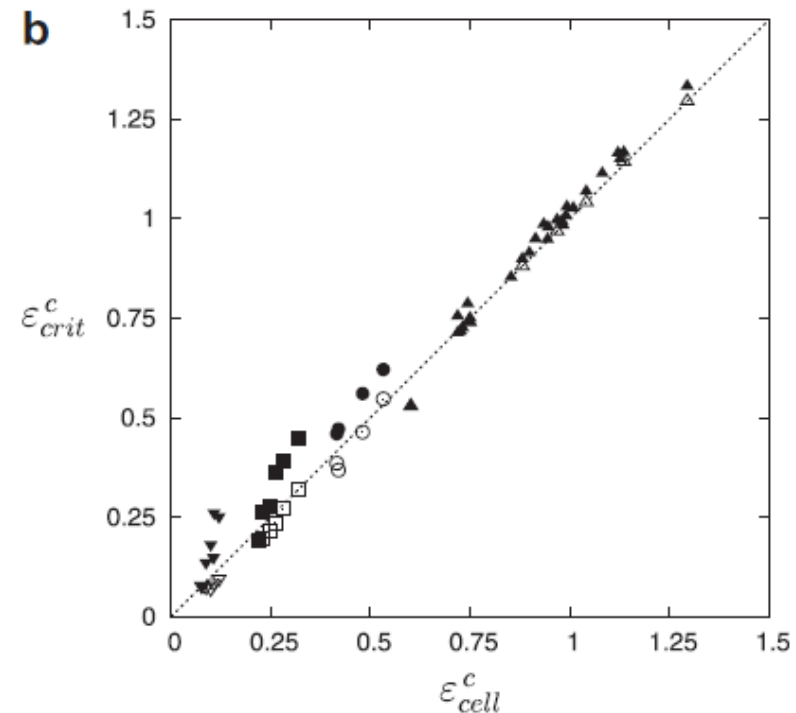
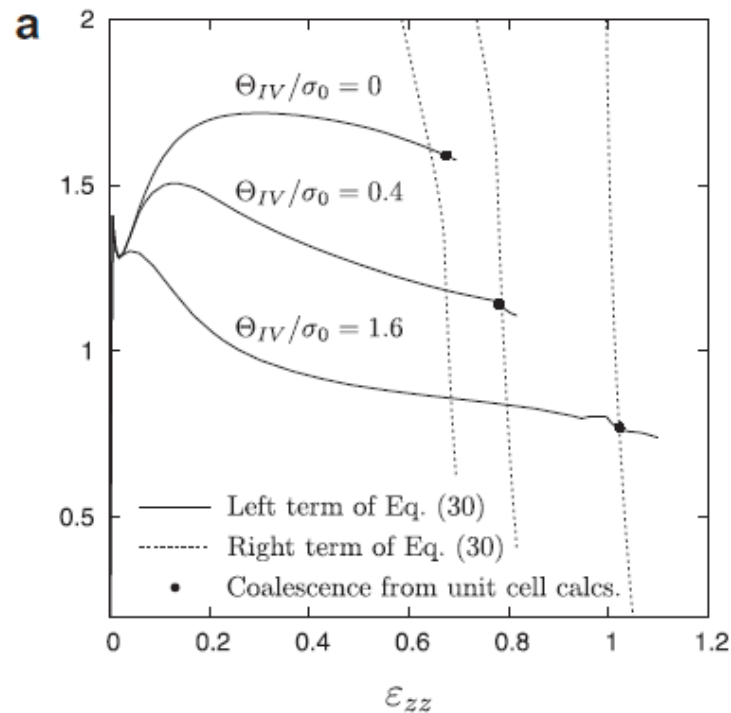


$$\sigma_y = \begin{cases} \sigma_0 + \frac{\Theta_0}{\beta} [1 - \exp(-\beta \epsilon_{acc}^p)] & \text{for } \sigma_y \leq \sigma_y^{tr} \quad (\text{stage III}) \\ \sigma_y^{tr} + \Theta_{IV} (\epsilon_{acc}^p - \epsilon_{acc}^{p-tr}) & \text{for } \sigma_y > \sigma_y^{tr} \quad (\text{stage IV}) \end{cases}$$

Works well when using the current incremental  $n_\varepsilon$  strain hardening value in

$$\alpha(n) = 0.1 + 0.217n + 4.83n^2 \quad (0 \leq n \leq 0.3)$$

$$\frac{\sigma_{zz}}{\sigma_y} = (1 - \chi^2) \left[ \alpha(n_\varepsilon) \left( \frac{1 - \chi}{\chi W} \right)^2 + 1.24 \frac{1}{\sqrt{\chi}} \right].$$



## Second approach (2008-2009)

$$\frac{\sigma_z}{\sigma_y^{loc}} = (1 - \eta\chi^2) \left[ 0.1 \left( \frac{1 - \chi}{\chi W} \right)^2 + 1.24 \sqrt{\frac{1}{\chi}} \right]$$

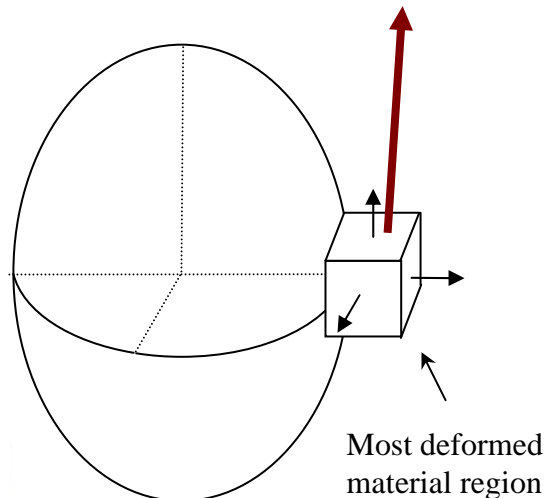
Localization is controlled by the local value of the yield stress

constant again !

$$\epsilon_y^{ploc} = \int \sqrt{\frac{2}{3} \dot{\epsilon}_{ij}^{ploc} \dot{\epsilon}_{ij}^{ploc}} dt$$

hardening law

$$\sigma_y^{loc}$$



$$\dot{\epsilon}_{33}^{ploc} = \frac{\dot{R}_3}{R_3} = \frac{1}{3} \left( \frac{\dot{f}}{f} - \frac{\dot{W}}{W} + \dot{\epsilon}_{22}^{\infty} + \dot{\epsilon}_{11}^{\infty} \right)$$

$$\dot{\epsilon}_{22}^{ploc} = \frac{\dot{R}_2}{R_2} \frac{P_e}{4R_2} \approx \frac{1}{3} \left( \dot{\epsilon}_{22}^{\infty} + \dot{\epsilon}_{11}^{\infty} + \frac{\dot{f}}{f} + 2 \frac{\dot{W}}{W} \right) \left( \frac{\pi}{2} \sqrt{\frac{1}{2} \left( \frac{1}{W^2} + 1 \right)} \right)$$

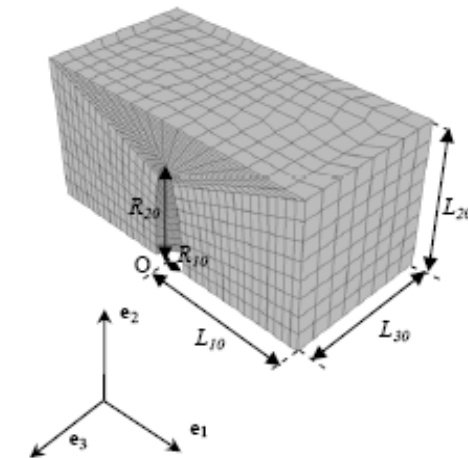
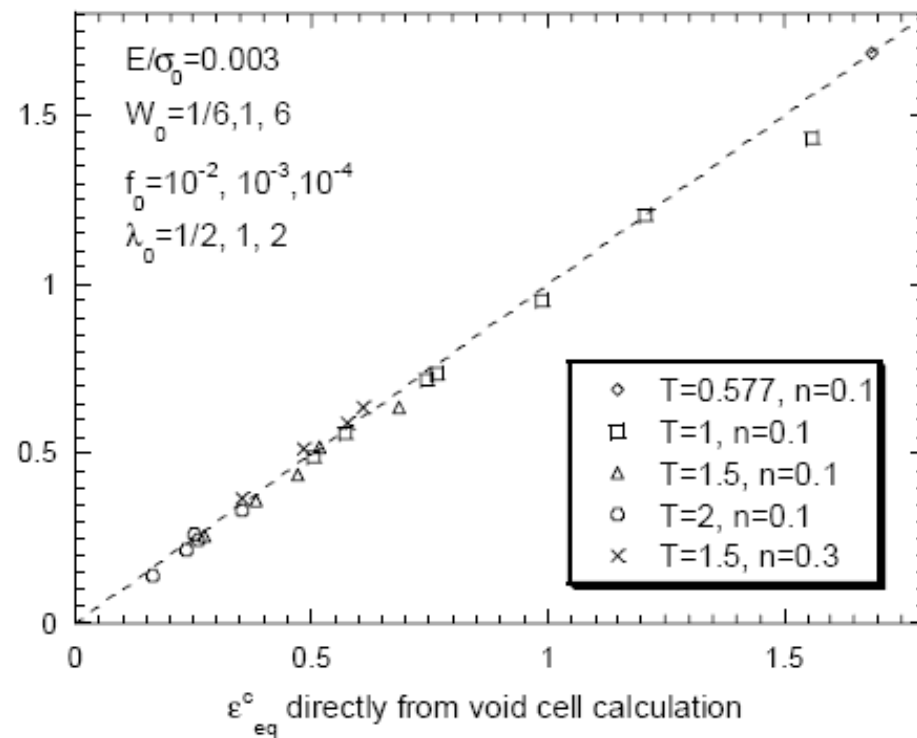
$$\dot{\epsilon}_{11}^{ploc} = -\dot{\epsilon}_{22}^{ploc} - \dot{\epsilon}_{33}^{ploc}$$

*Kinematic model very accurate !*

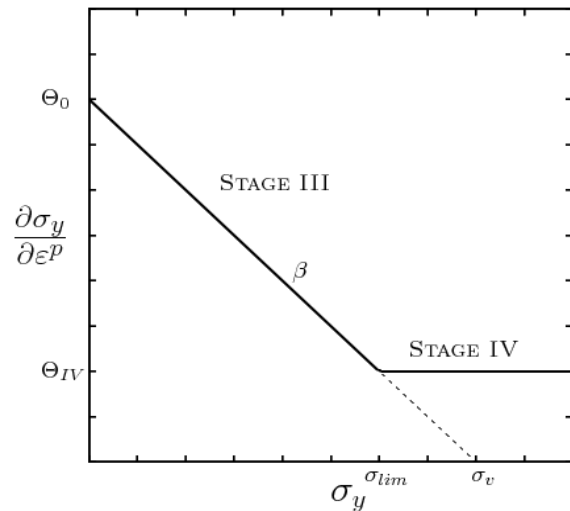
## Validation 1 : for power law hardening

$$\sigma_y = \sigma_0 \left( 1 + \frac{\varepsilon_y^p}{\varepsilon_0} \right)^n$$

$\varepsilon_{eq}^c$  with local yield stress



## Validation 2 : Voce law with stage IV

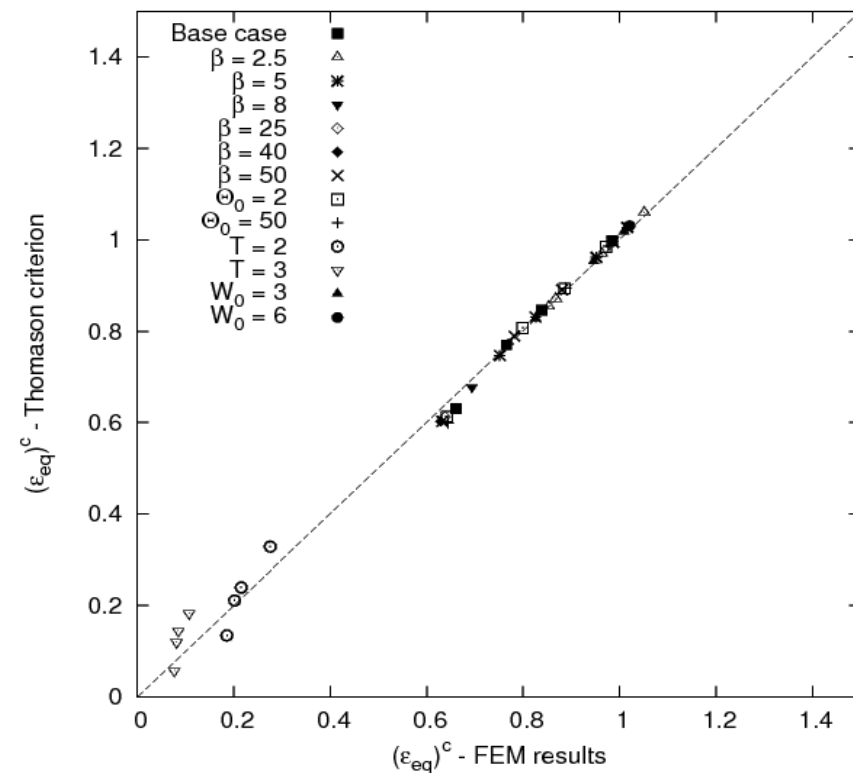


$$\sigma_y = \sigma_0 + \frac{\Theta_0}{\beta} [1 - \exp(-\beta \cdot \varepsilon^P)] \quad [\text{stage III}]$$

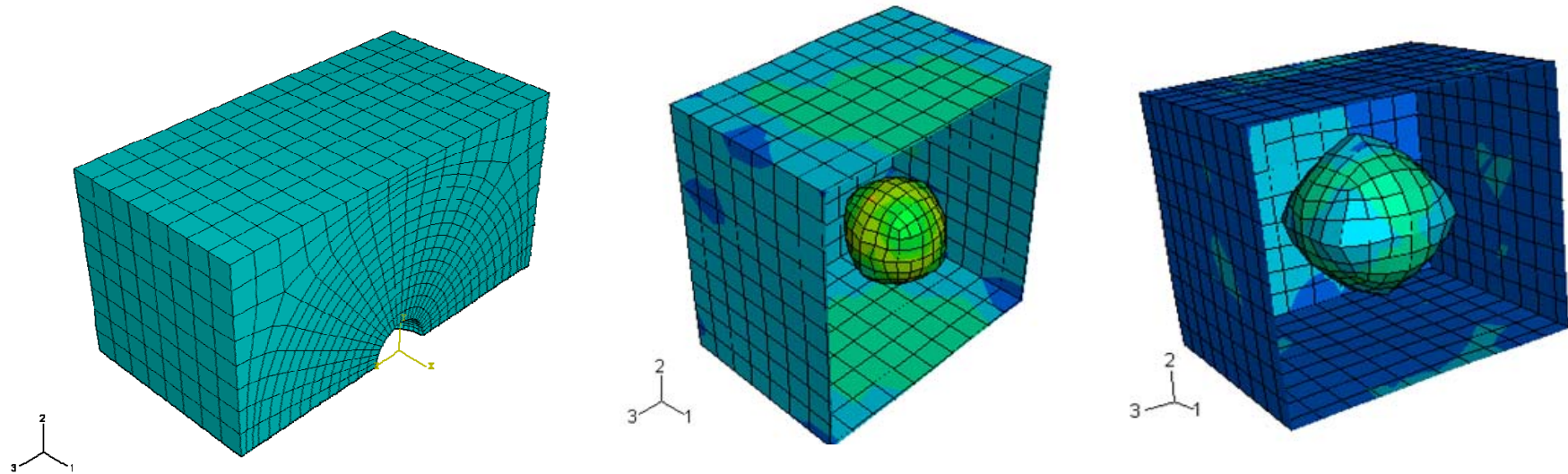
$$\sigma_y = \sigma_{lim} + \Theta_{IV} \cdot (\varepsilon^P - \varepsilon_{lim}^P) \quad [\text{stage IV}]$$

Excellent agreement  
with FE void cell  
simulations except at  
high triaxiality

Equivalent strain at coalescence - From FEM results and Thomason criterion



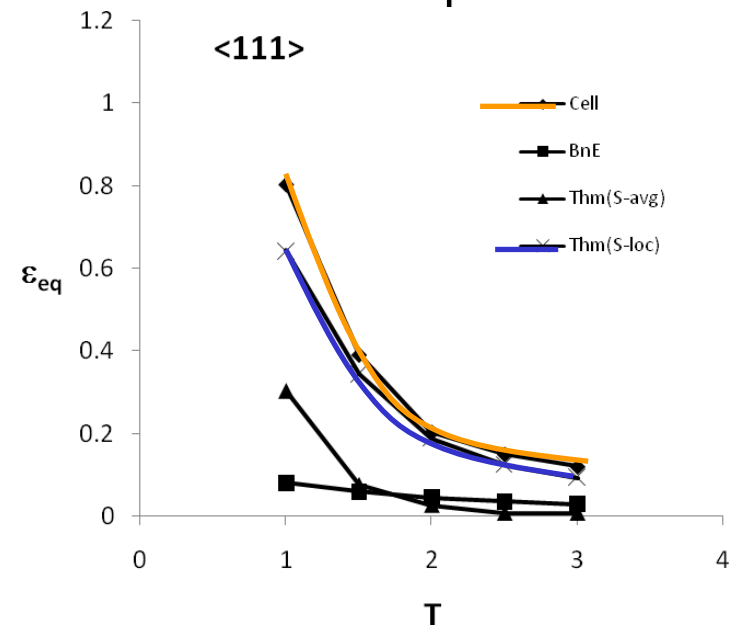
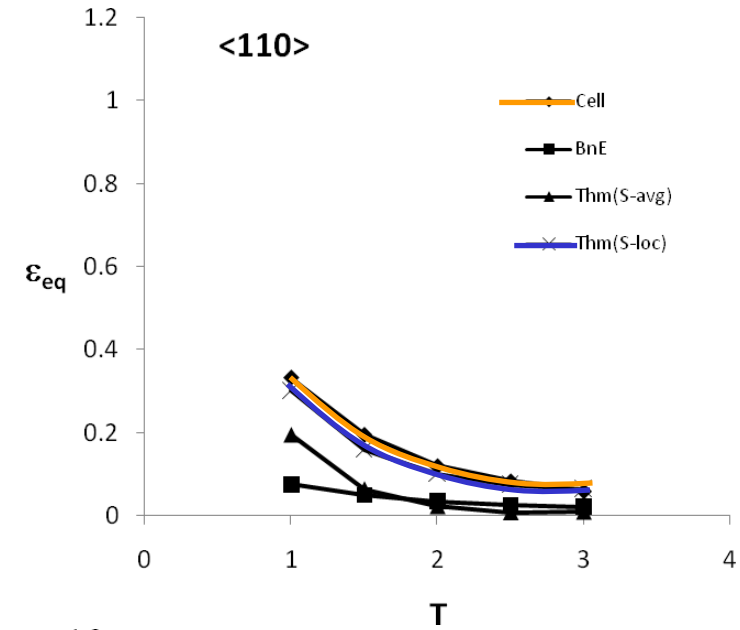
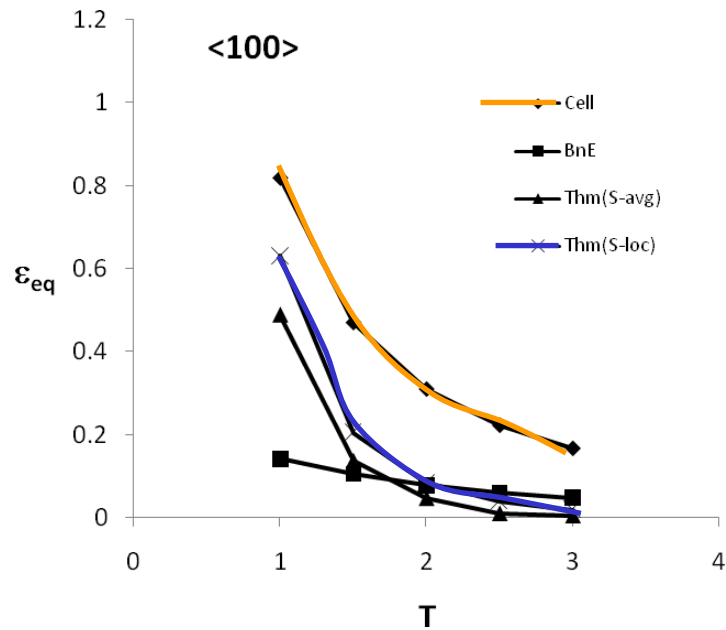
## Validation 3 : single crystal plasticity with power law hardening



3D void cell simulations (Abaqus)  
Fully periodic BC  
Constant stress triaxiality  
BCC single crystal (48 slip systems)  
Different crystal orientation  
Power law hardening for CRSS

$$\tau_c = \tau_{co} \left( 1 + \frac{\Gamma}{\Gamma_o} \right)^n$$

## Assessment of new Thomason criterion with local yield stress



**Works very well**  
... except for <100> at high triax  
(local shear strain not taken into  
account)



# OUTLINE

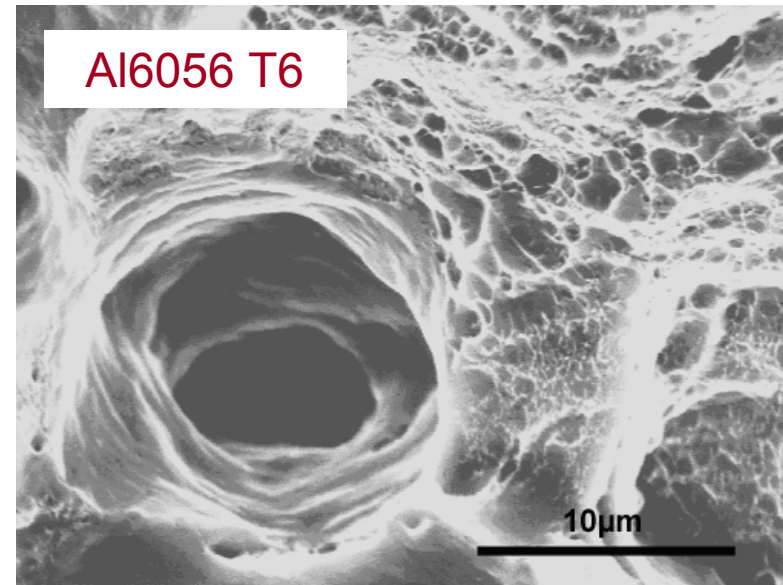
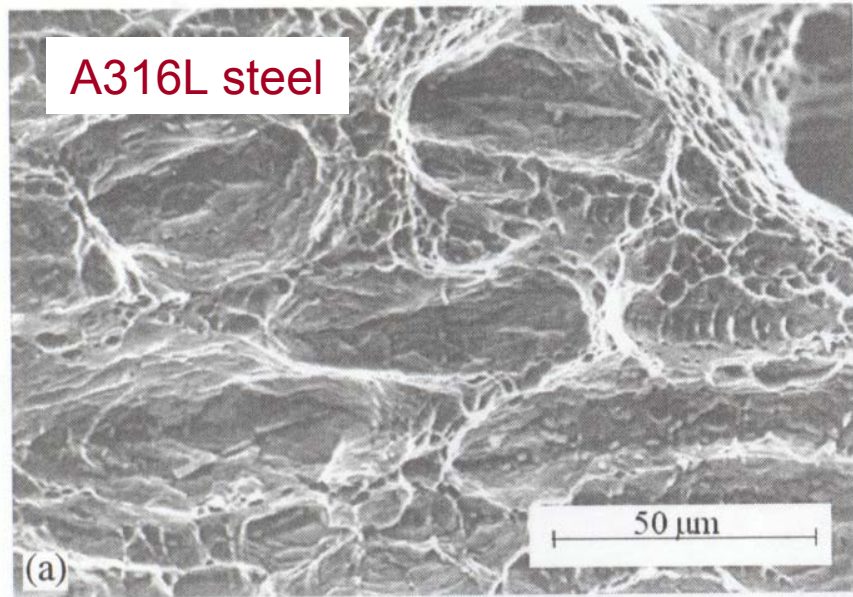
1. Experimental observations
2. « Elementary » models for the onset of void coalescence
3. Fine tuning of Thomason model
4. Extension to strain hardening
- 5. Extension to a second population**
6. Extension to combined shear/tension coalescence
7. Models for the coalescence stage



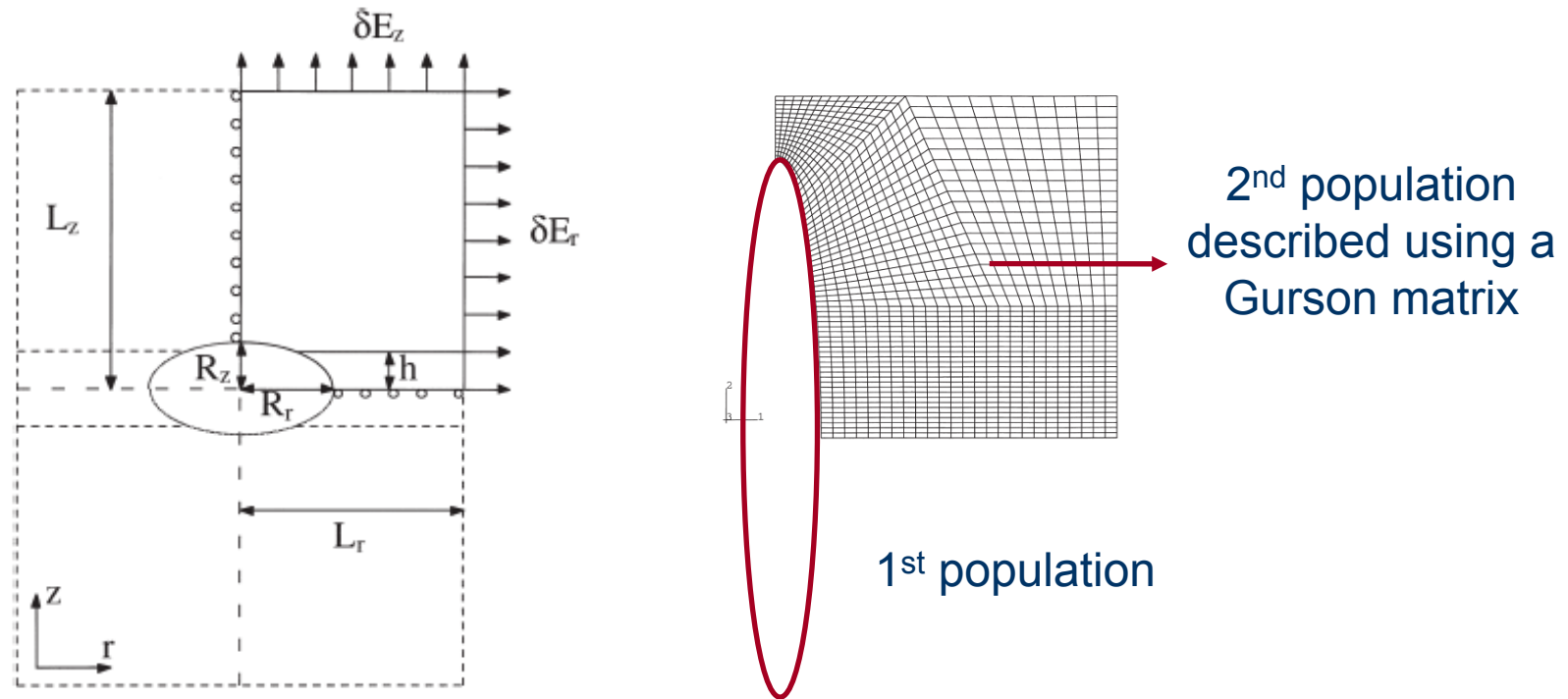
## Secondary voids are often observed on fracture surfaces of metallic alloys

Second populations of voids result from nucleation on submicron sized particles at large strains, e.g.

- carbides in steel
- dispersoids in Al alloys
- small  $\alpha$  particles in  $\alpha/\beta$  Ti alloys

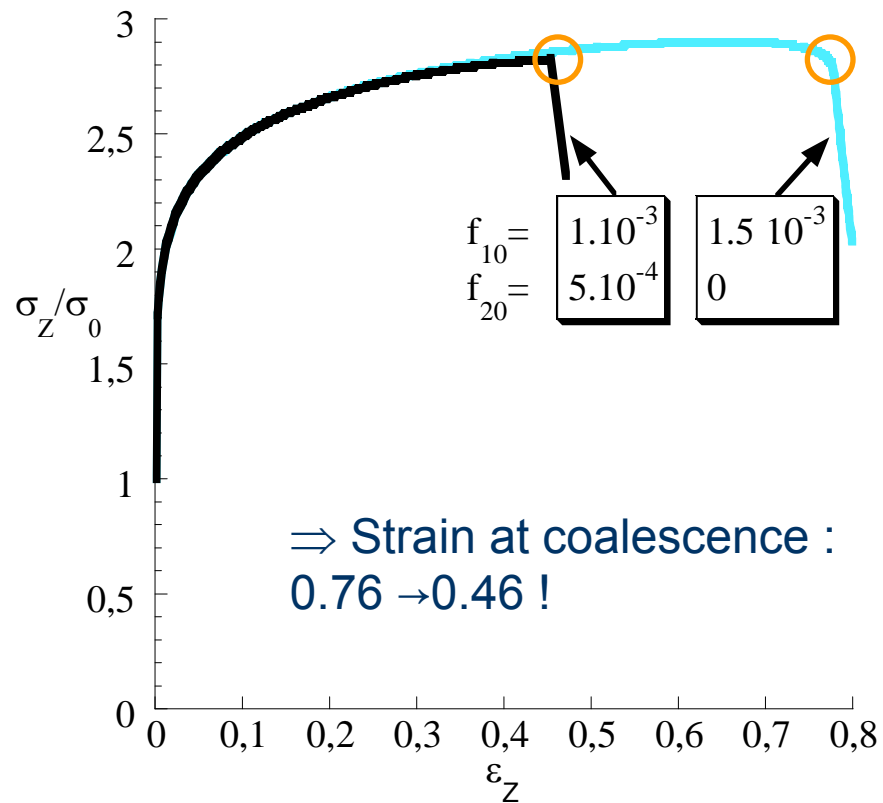


## FE void cell calculations with two populations of voids



2D axisym void cell simulations (Abaqus)  
 Periodic BC & constant stress triaxiality  
 Gurson matrix  
 Different primary and secondary void vol. fr.  
 Primary voids already present  
 Strain controlled nucleation of secondary voids

## Major influence of the presence of a second population on the onset of void coalescence, but no effect on the growth of the primary voids



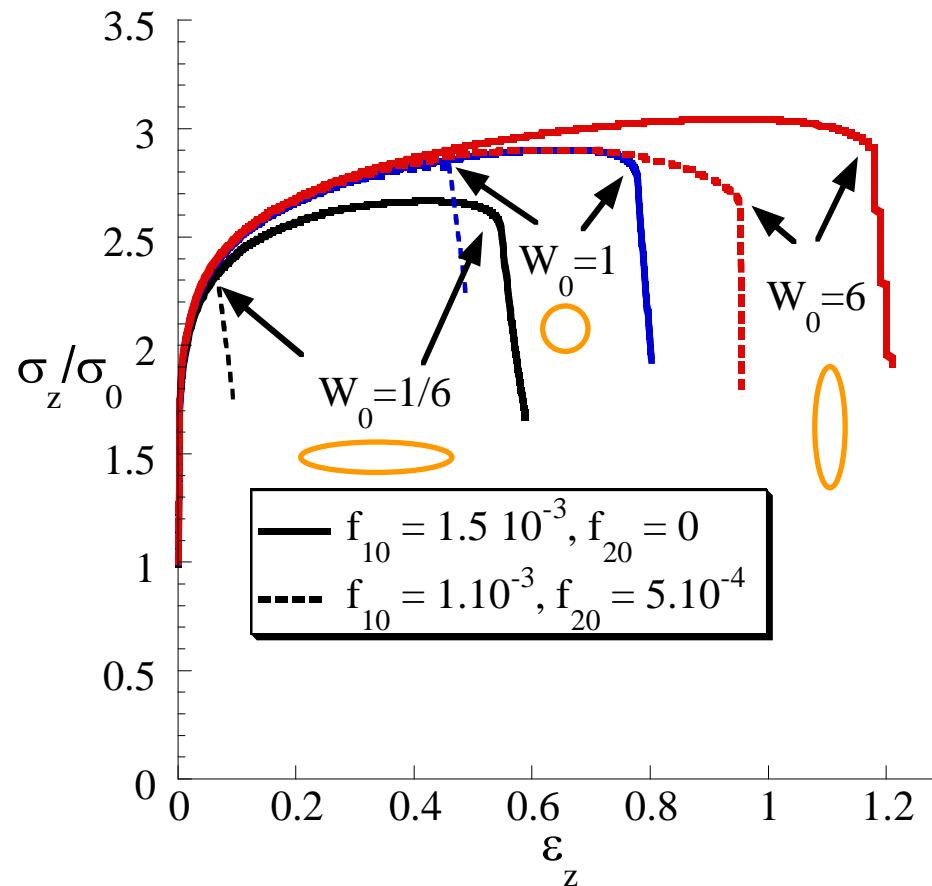
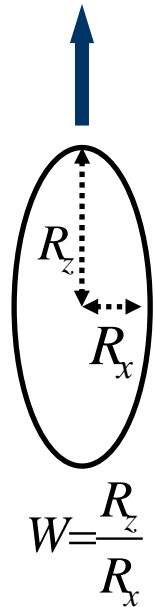
Triaxiality = 1  
 2<sup>nd</sup> population present from the beginning  
 1<sup>st</sup> population spherical

$$E/\sigma_0 = 500$$

$$n = 0.1$$



## The effect of the presence of secondary voids on triggering coalescence is much larger with flat voids

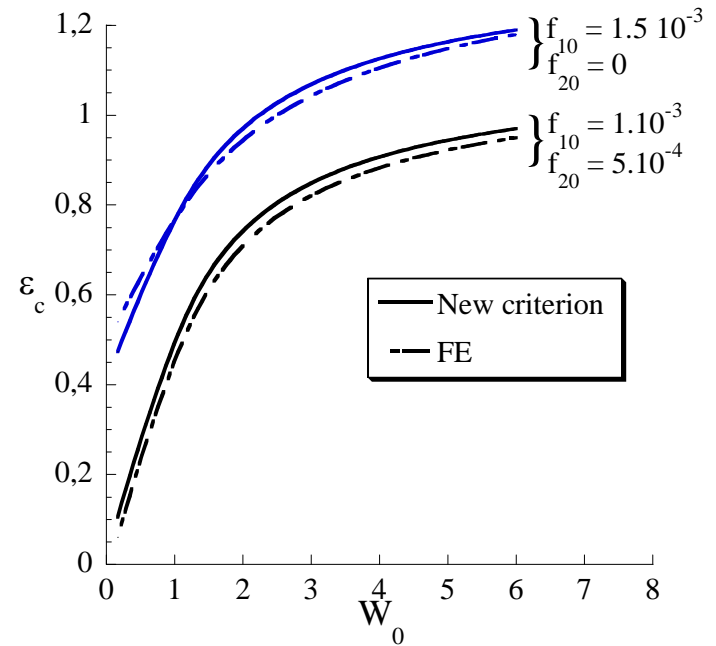
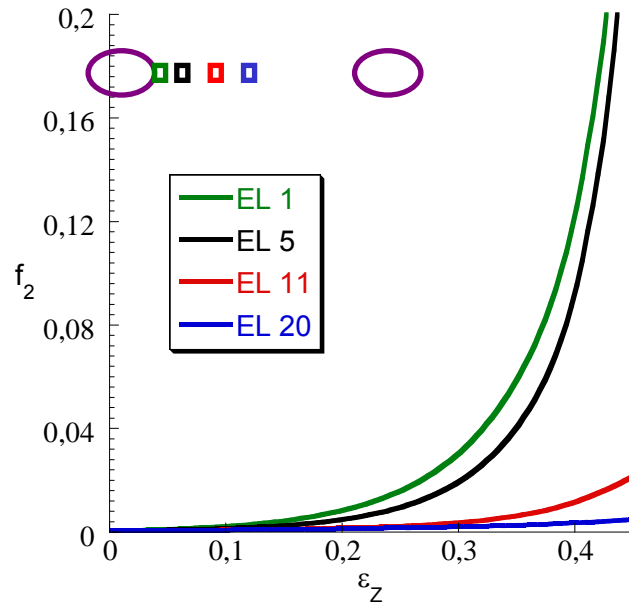
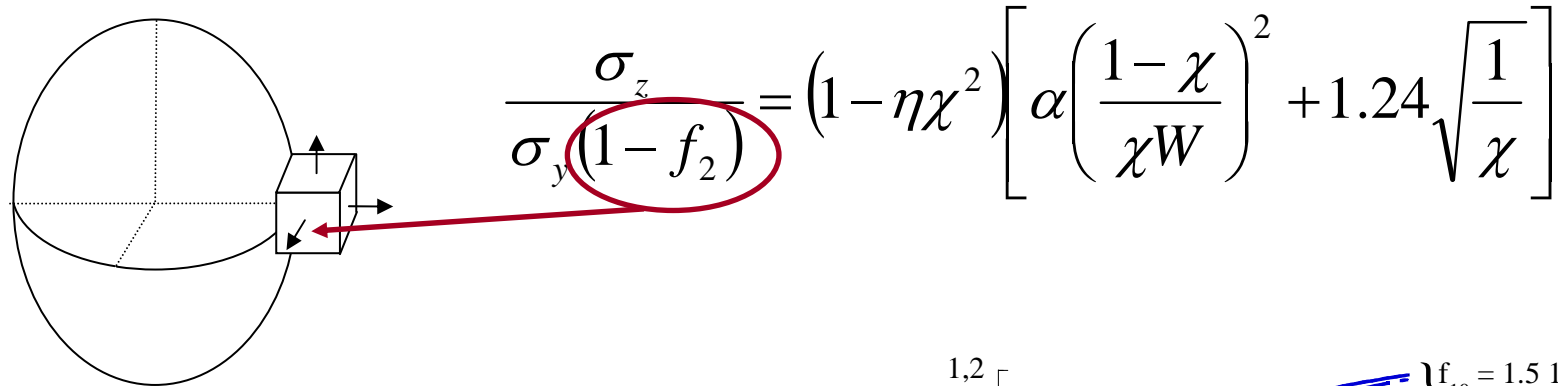


Triaxiality = 1  
2<sup>nd</sup> population  
present from the  
beginning

$$E / \sigma_0 = 500$$

$$n = 0.1$$

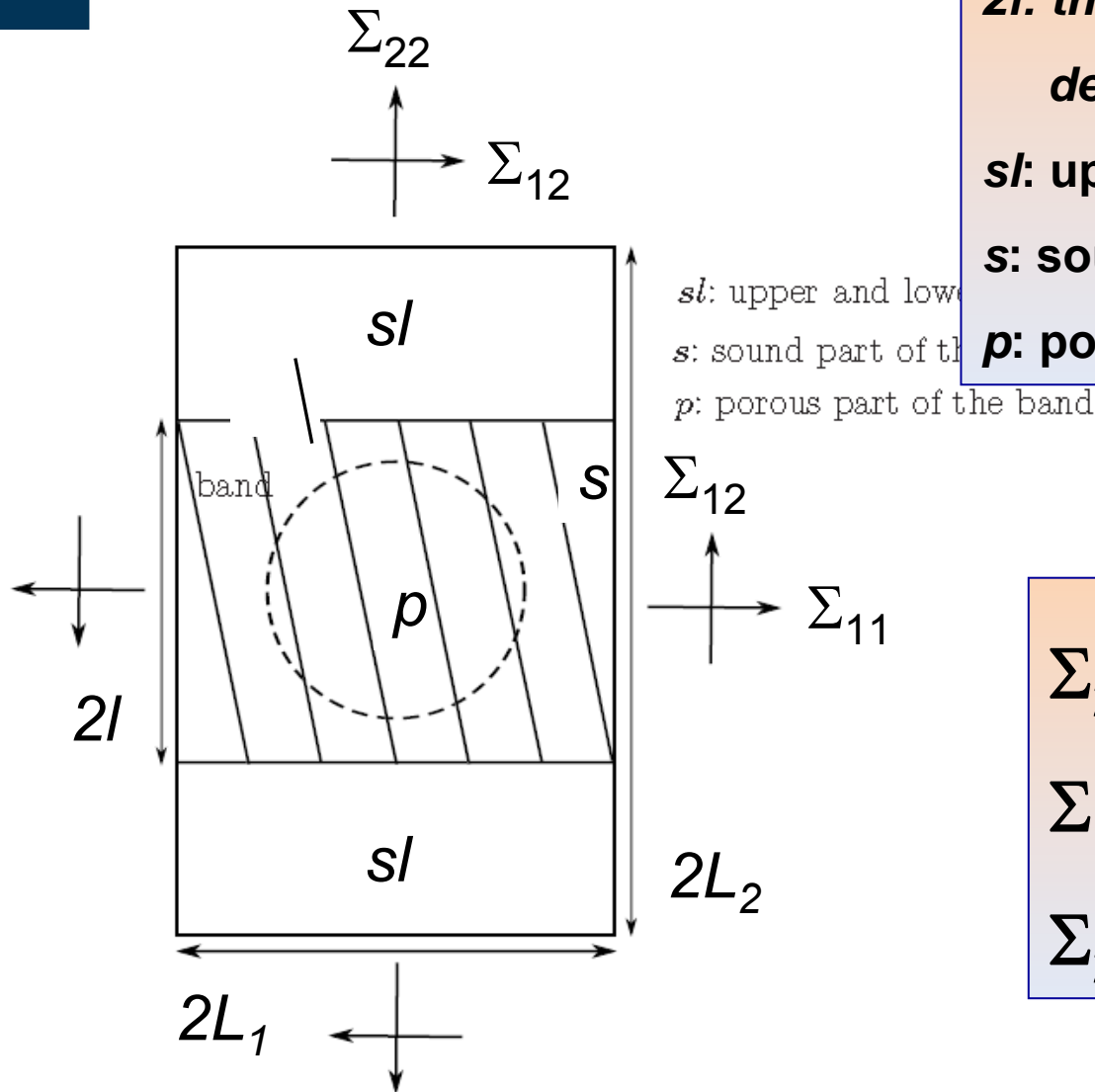
## Introduce second population in the void coalescence criterion



# OUTLINE

1. Experimental observations
2. « Elementary » models for the onset of void coalescence
3. Fine tuning of Thomason model
4. Extension to strain hardening
5. Extension to a second population
- 6. Extension to combined shear/tension coalescence**
7. Models for the coalescence stage

# Coalescence Criterion for General Loadings



***2l***: the thickness of the localized deformation band

***sl***: upper and lower sound layers

***s***: sound part of the band

***p***: porous part of the band

$$\Sigma_{22} > \Sigma_{11}; \Sigma_{22} > \Sigma_{33}$$

$$\Sigma_{12} = \Sigma_{21} \neq 0$$

$$\Sigma_{23} = \Sigma_{32} \neq 0$$



# Critère de coalescence de Thomason étendu



*Slide venant  
de Jean-  
Baptiste*

$$\left( \frac{\Sigma_{22}}{\Sigma_{22}^{Th}} \right)^2 + \frac{3(\Sigma_{21}^2 + \Sigma_{23}^2)}{(1 - f_b)^2 \sigma_0^2} = 1$$

$\Sigma_{22}^{Th}$  : « contrainte de coalescence » en traction pure donnée par Thomason

$f_b = f \frac{L_2}{\ell}$  : porosité dans la bande

( $\ell$  est prise proportionnelle à la dimension verticale du vide)

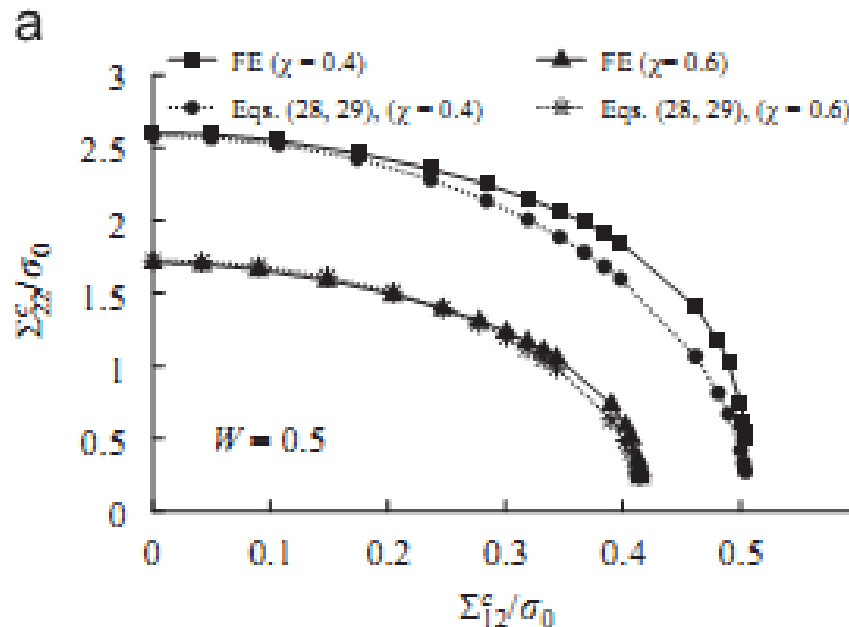
# Comparaison avec des simulations numériques micromécaniques



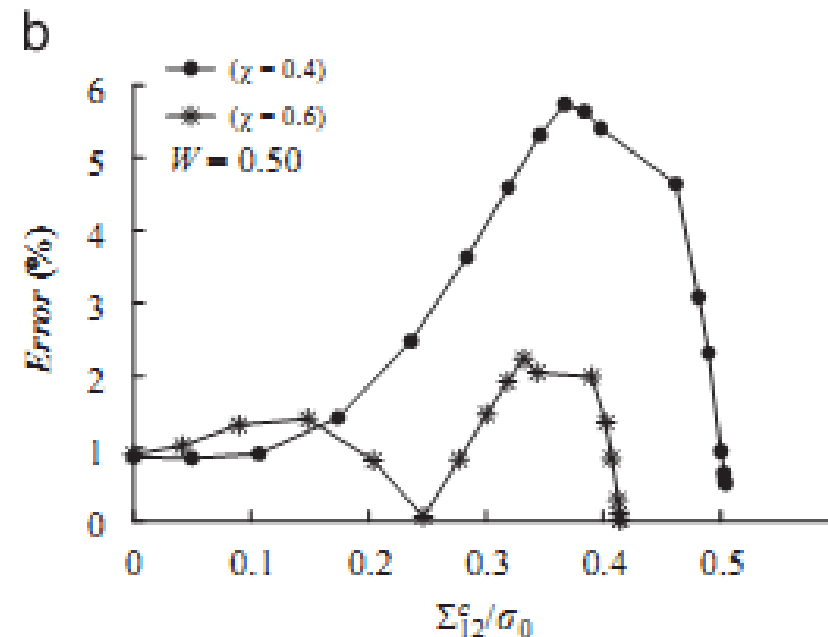
Meilleur accord quand

$2l = 0.6R_2$ , corresponding to an  $f_b$  value of

$$f_b = 1.455 \frac{L_2}{R_2} f = 1.455 \frac{L_2}{\chi W L_1} f.$$



a: critères de coalescence analytique et numérique



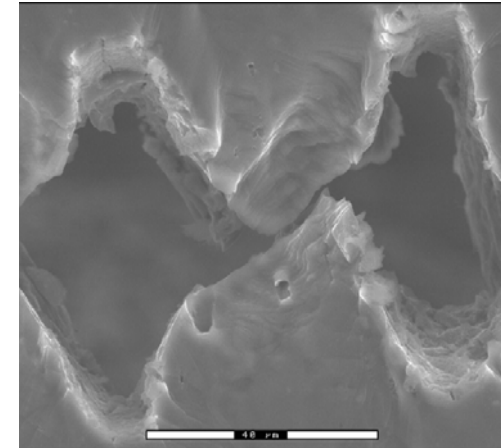
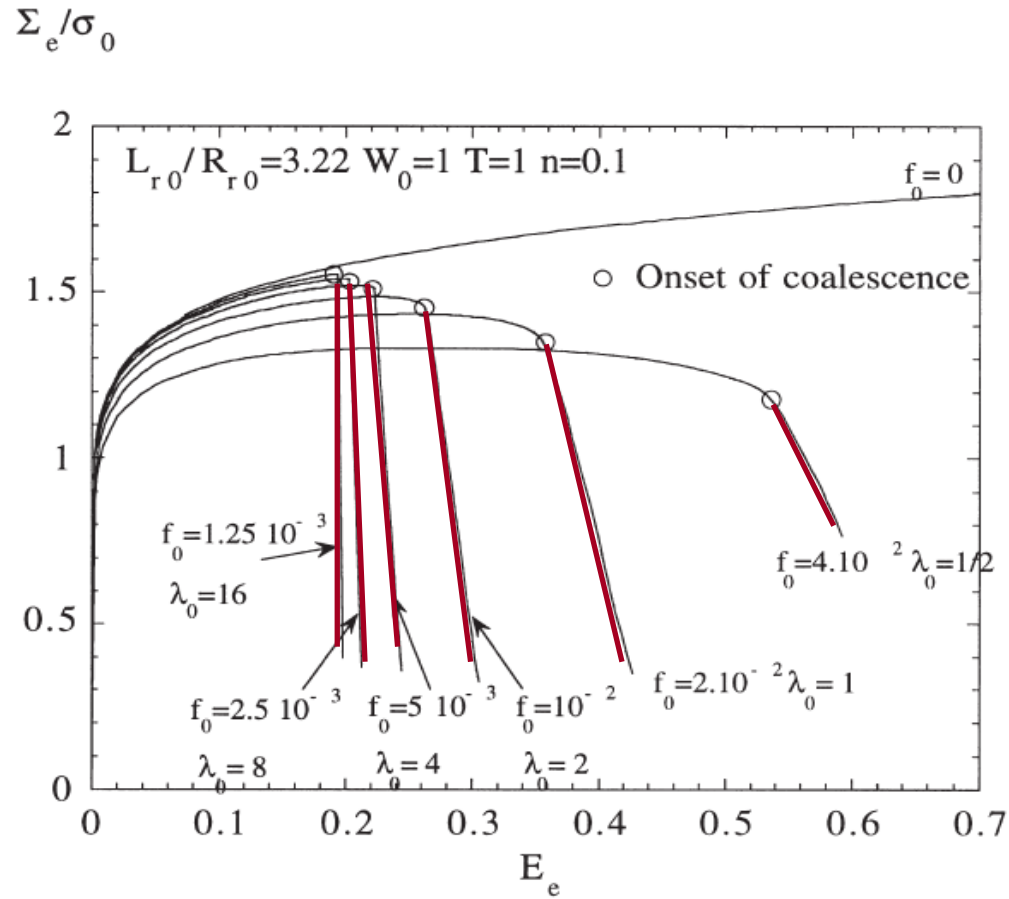
b: erreur relative



# OUTLINE

1. Experimental observations
2. « Elementary » models for the onset of void coalescence
3. Fine tuning of Thomason model
4. Extension to strain hardening
5. Extension to a second population
6. Extension to combined shear/tension coalescence
- 7. Models for the coalescence stage**

# Models for the coalescence stage

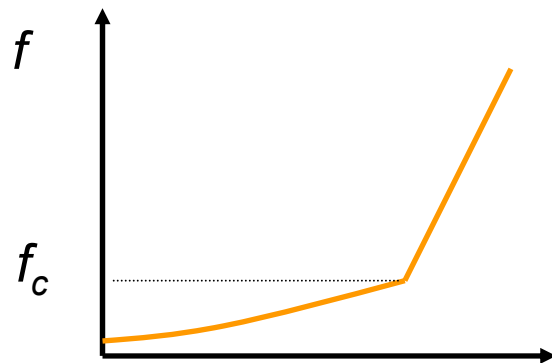


Weck et al.

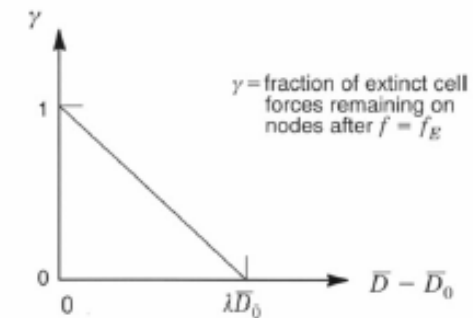
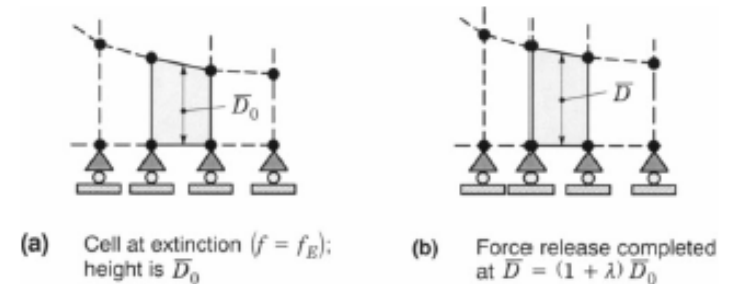
## Standard approaches

In the framework of Gurson model introduce an artificial acceleration factor for the porosity growth (Tvergaard and Needleman, 1984)

$$f^* = \begin{cases} f & \text{if } f < f_c \\ f_c + \delta(f - f_c) & \text{if } f \geq f_c \end{cases}$$

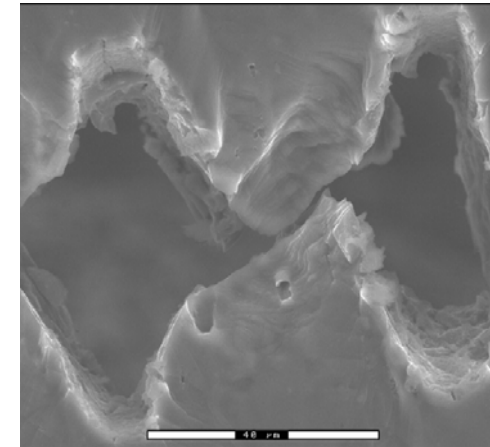
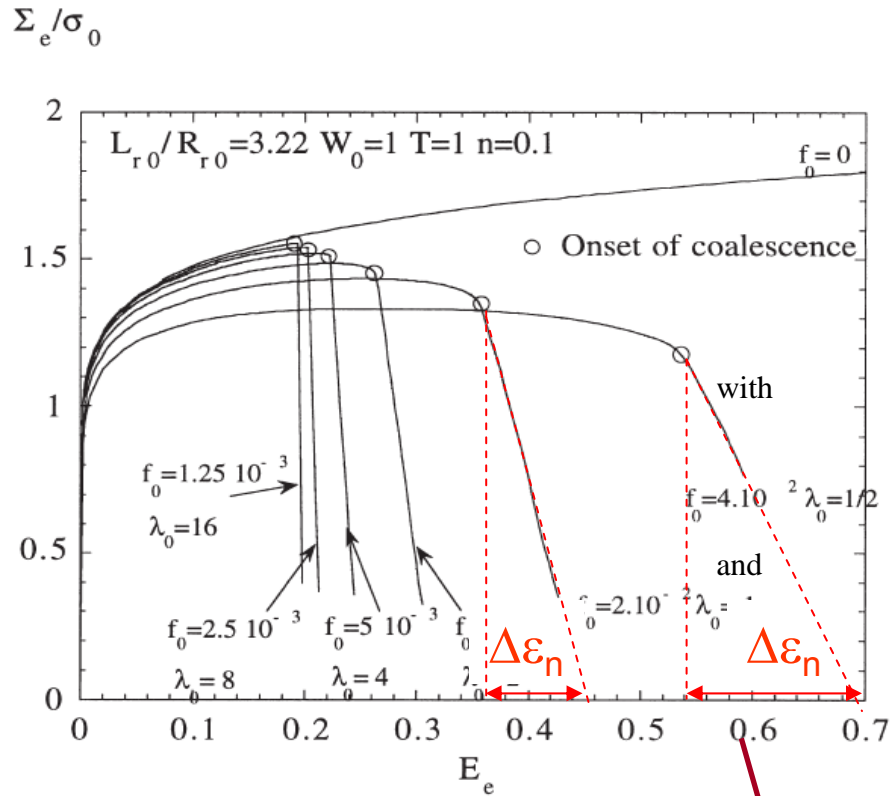


or  
Prescribe unloading slope via a sort of cohesive zone model (Shih, Dodds, ...)



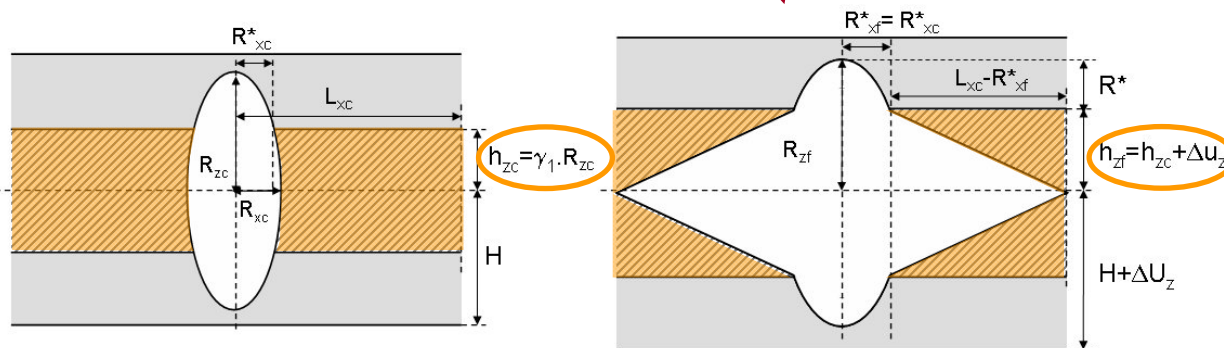
(c) Linear traction-separation model

# « geometric » approach



Weck et al.

$$\Delta \epsilon_n = F(\chi_c, W_c, \text{strain state})$$



# Full constitutive model approach

*Let's think in terms of two yield surfaces*

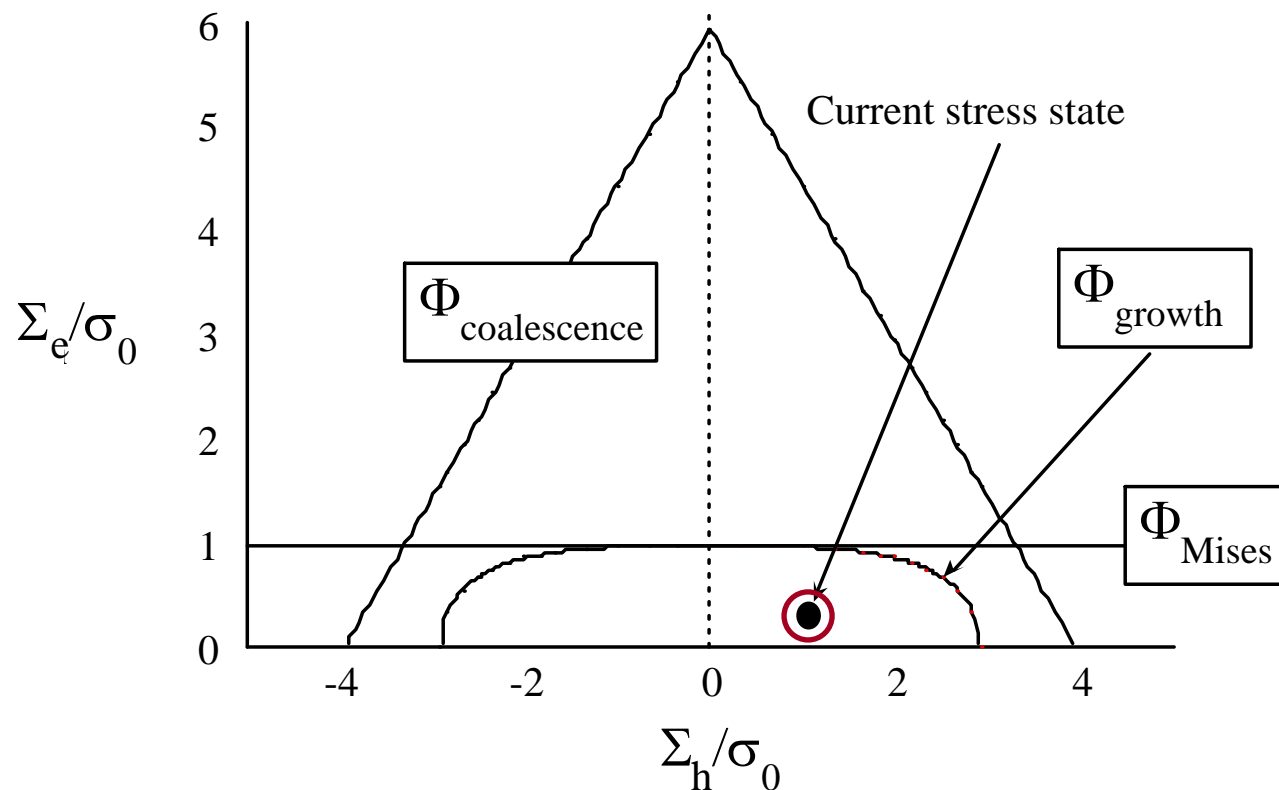
$$\Phi_{\text{coalescence}} \equiv \frac{\Sigma_e}{\sigma_f} + \frac{1}{2} \frac{\Sigma_{kk}}{\sigma_f} - F(S, \chi) = 0$$

See Benzerga or Pardoen and Hutchinson

+ evolution laws for the internal variables

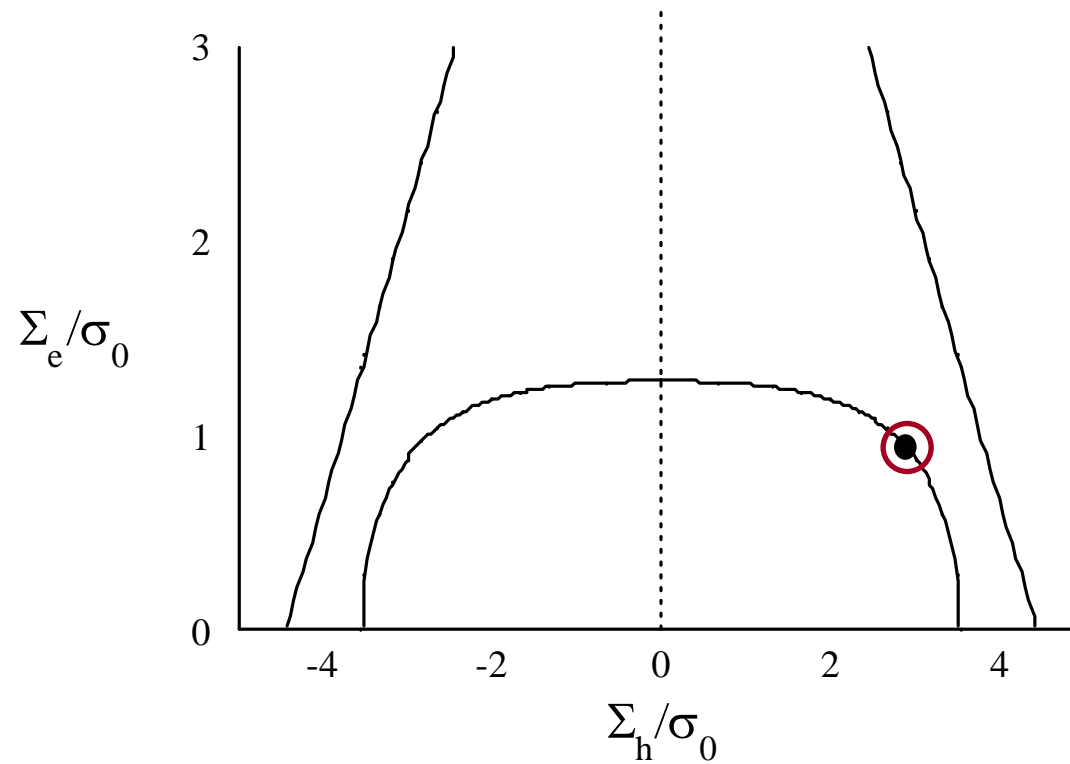
**Elasticity**

$$F(W, \chi) \equiv \frac{3}{2} (1 - \eta \chi^2) \left[ \alpha \left( \frac{1 - \chi}{\chi W} \right)^2 + \beta \sqrt{\frac{1}{\chi}} \right]$$



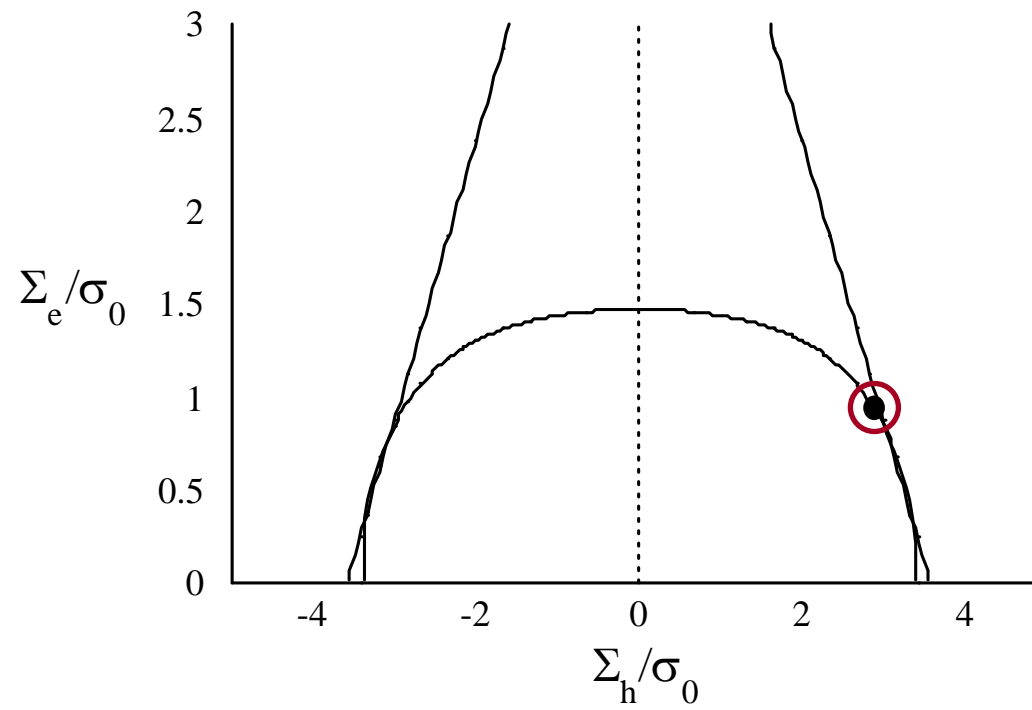


## First, void growth, but strain hardening dominates damage softening



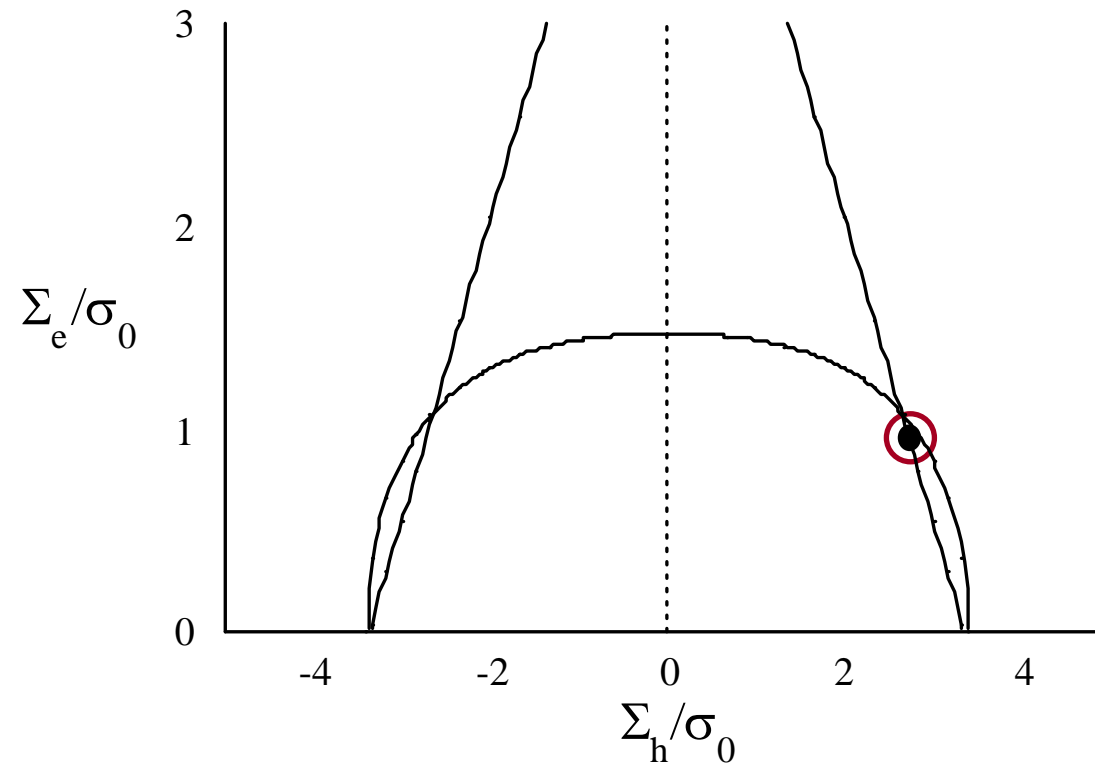


## Just before void coalescence



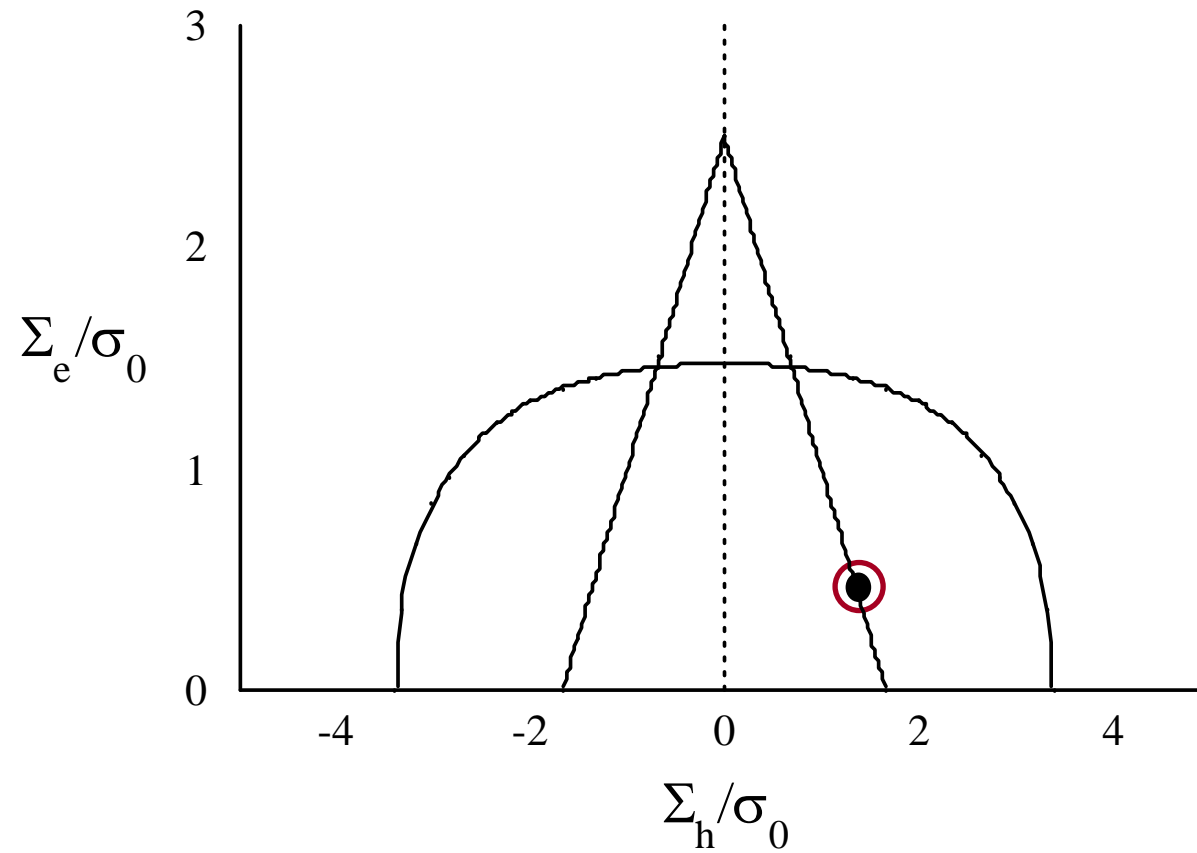


## Just after the onset of void coalescence



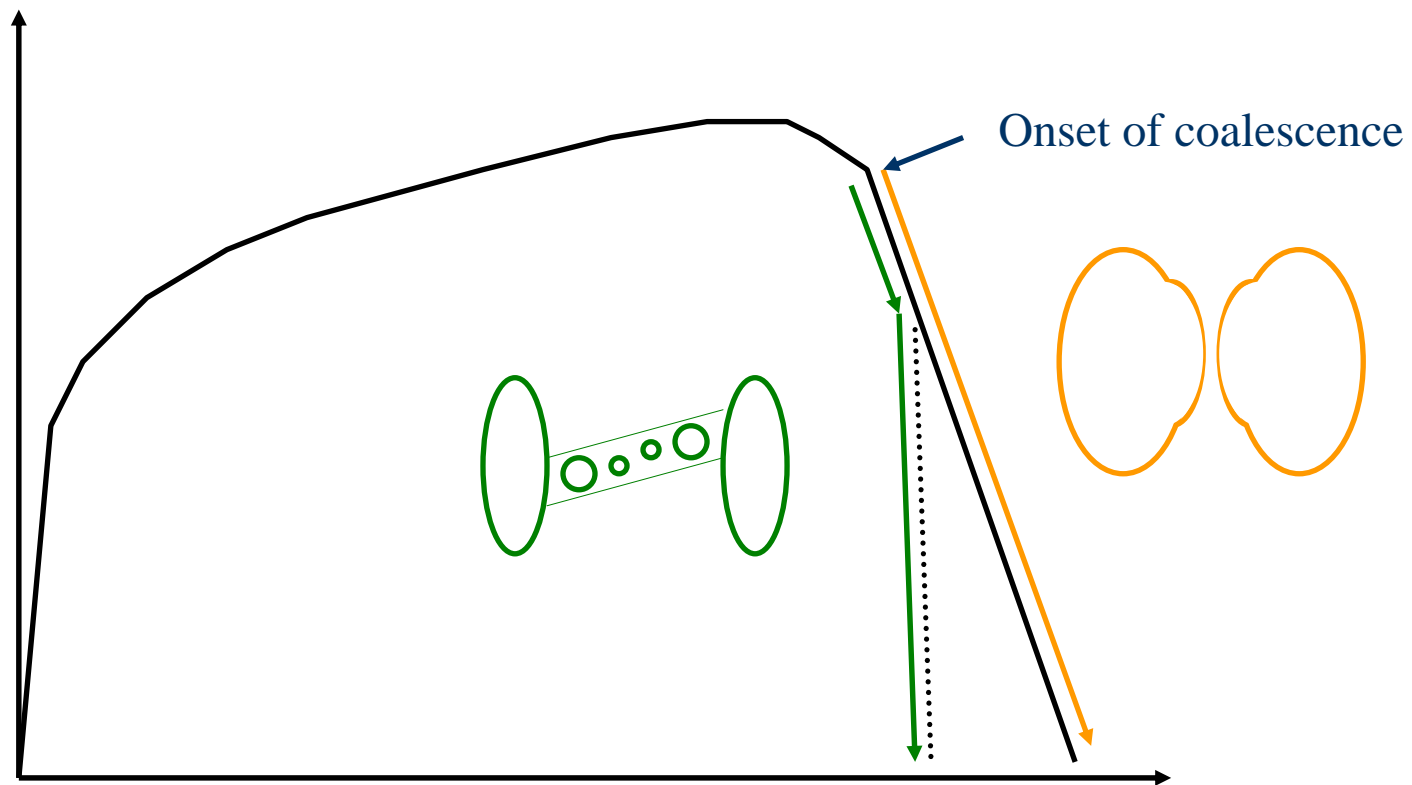


## During the coalescence phase





## Additional effects taking place during coalescence



See e.g. Fabrègue and Pardoën, 2008

# Conclusion

**No time for conclusions !!!**